

23 MEI 1953

REPORT No. 69

TECHNISCHE UNIVERSITEIT DELFT  
LUCHTVAERT EN FLUGTECHNIJK  
Luchtvaarttechniek  
Kluyverweg 1 - 2629 HS DELFT

THE COLLEGE OF AERONAUTICS  
CRANFIELD



SOME EXPERIMENTS ON THE FLOW IN THE  
BOUNDARY LAYER OF A 45° SWEEPBACK  
UNTAPERED WING OF ASPECT RATIO 4.

by

K. EMSLIE, D.C.Ae.

L. HOSKING, D.C.Ae.

W. S. D. MARSHALL, D.Ae.(Hull), A.F.R.Ae.S.

February, 1953

THE COLLEGE OF AERONAUTICS  
C R A N F I E L D

Some Experiments on the Flow in the Boundary Layer of  
a  $45^{\circ}$  Sweptback Untapered Wing of Aspect Ratio 4.\*

-by-

K. Emslie, D.C.Ae.,

L. Hosking, D.C.Ae.,

and

W.S.D. Marshall, D.Ae. (Hull), A.F.R.Ae.S.

-----  
SUMMARY

Visual methods have been used together with a yawmeter to illustrate conditions of flow in the boundary layer over a sweptback wing. It was found that at moderate incidences a marked outflow in the boundary layer was developed. At higher incidences (about  $16^{\circ}$ ) what appears to be laminar separation with reattachment occurred at the leading edge near the root; this manifests itself as a standing vortex. At a somewhat lower incidence ( $12^{\circ}$ ) a region of separated flow in the turbulent boundary layer developed at the trailing edge. The extent of this region was found to increase with increase of incidence. Boundary layer thickness was found to increase rapidly towards the trailing edge and slightly as the tip was approached. When the angle of outflow became equal to the angle of sweepback (i.e. the chordwise flow was on the point of separation) the spanwise boundary layer profiles showed marked deviation from the  $1/7$ th power law, but at lower incidences the spanwise flow profiles approximately followed this law.

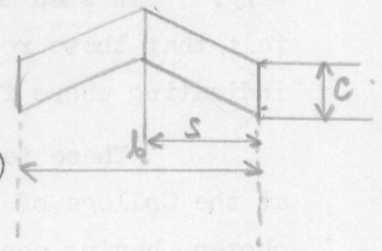
MEP

---

\* Most of the work described in this report was described by the first two authors in a report submitted in part fulfilment of the requirements for the award of the College Diploma.

NOTATION

- $\alpha$  Angle of incidence
- $x$  Distance aft of leading edge
- $y$  Spanwise distance from  $\zeta$  of wing
- $z$  Distance from surface, measured normal to surface
- $c$  Length of the chord
- $s$  Semi-span
- $\eta$  Non-dimensional spanwise distance ( $= y/s$ )
- $\delta$  Boundary layer thickness
- $U$  Local velocity outside boundary layer
- $u_r$  Local velocity inside boundary layer
- $u$  Chordwise component of velocity (normal to leading edge)
- $v$  Spanwise component of velocity (parallel to leading edge)
- $q$  Local dynamic head  $= \frac{1}{2} \rho u_r^2$
- $p$  Local static pressure
- $H$  Local total head.
- $p_1, p_2$  Pressures recorded in the tubes of the yawmeter
- $R_1 = \frac{p_1 - p}{q}$
- $R_2 = \frac{p_2 - p}{q}$
- $\epsilon$  Angle between yawmeter axis and local direction of flow
- (H) Angle of local flow to free stream direction



Suffix  $o$  refers to free stream values.

## 1. Introduction

This paper describes one of a series of investigations into the aerodynamic characteristics of swept back wings at low speeds that are being made at the College of Aeronautics. A previous paper<sup>4</sup> described the results of measurements of pressure distributions with trailing edge split flaps; this paper is concerned with measurements of the boundary layer on a swept back wing. Few such measurements have been made to date, and it was felt that these results should be of interest particularly in indicating where future research should be directed.

These tests were made in 1951-2 in the No. 2 Wind Tunnel at the College of Aeronautics. For these tests a simple wing was chosen, having constant chord and no twist, and the object of the test was to provide data, both qualitative and quantitative, on the flow in the boundary layer, and for this purpose visual and direct measurement techniques were used.

## 2. Details of Apparatus and Techniques

### 2.1. General Details

The model used was constructed of laminated mahogany. It represented a wing whose chord was constant. The span was 30 in. and the aspect ratio was 4. The aerofoil section parallel to the free stream direction was 10 per cent thick and symmetrical. The maximum thickness occurred at 30 per cent of the chord aft of the leading edge and the section had an elliptical nose and a straight trailing edge.

The model was suspended from the balance in the No. 2 Wind Tunnel, and the tunnel speed for all tests was approximately 130 ft/sec. corresponding to a Reynolds number of  $0.52 \times 10^6$  based on wing chord.

The photographs were taken with a simple 35mm camera placed on circular arc track in the plane of symmetry of the model. This enabled undistorted pictures of the wing to be taken over a wide range of incidence and yaw.

### 2.2. Tuft Technique

Nylon threads 1.1 in. long were glued to the tops of pins to investigate the local directions of flow at various distances from the wing surface. The pins were tapped into the surface of the wing at 28 spanwise positions and spaced along chord lines at positions staggered between port and starboard wings as shown in fig. 1. The pins were cut first at  $3/4$  in. from the surface and

/the tufts ...

the tufts were glued to them so that the tufts trailed approximately downstream. The behaviour of the tufts was observed over a wide range of angles of incidence including both positive and negative angles, giving in effect the flow patterns close to both upper and lower surfaces. A limited number of tuft observations were also made with the model yawed.

The pins were cut off successively to  $1/2$ ,  $1/4$  and  $1/8$ in., and each time fresh tufts were glued on and the tests were repeated. Finally the pins were removed and the tufts stuck directly onto the wing surface.

Photographs were taken with the wind on and the resulting negatives were projected on to a ground glass screen. Tracings were taken showing the flow directions as streamlines, and the results for the various distances from the wing surface were collected for comparison. Incidences of  $8^\circ$ ,  $10^\circ$  and  $12^\circ$  were chosen as of most interest and the tracings were photographically reduced to produce figs. 2,3 and 4.

### 2.3. Lamp Black Technique

This method of flow visualisation due to Black (ref.1) was used to illustrate the flow pattern in the boundary layer immediately adjacent to the wing surface. Briefly, the technique consisted of spraying the surface of the wing uniformly with a suspension of lamp black in paraffin. The wing was then set to the required incidence and the tunnel speed was quickly adjusted. Then the spreading of the liquid left traces of lamp black along the streamlines of the boundary layer flow very close to the surface, and evaporation of the paraffin resulted in a pattern of lamp black which could be studied and photographed at leisure.

For proper interpretation of the dried pattern it was found desirable to have watched the formation of the pattern while the tunnel was running, noting the appearance of the surface of the liquid in motion in order to assess the relative speeds of the flow over different areas of the wing.

Photographs of the patterns together with explanatory diagrams are reproduced here as figs. 5 to 14.

### 2.4. Yawmeter Measurements

Traverses were made with a yaw meter to obtain quantitative measurements in the interesting regions indicated by the two visual techniques described above. The yaw meter head used in these tests consisted of two parallel tubes of 1mm diameter with the open ends

/chamfered ...

chamfered to an included angle of  $70^\circ$ . This type of yawmeter is due to O. Conrad of Göttingen, the first published data of which appeared in reference 2. This type of instrument is approximately twice as sensitive as a conventional claw type yawmeter, and, after calibration, it is possible to determine, in addition to the local direction of the flow, both static and dynamic pressures from a comparison of the readings in the two tubes. The method is described in the Appendix, where details are also given of the calibration.

The yawmeter was mounted on a turntable with the apex of the mouths of the tubes arranged to be on the axis of rotation of the turntable. A micrometer screw thread and barrel was incorporated in the system which enabled the level of the yawmeter to be altered in very small increments. Provision was made on the turntable itself for the position of the yawmeter head to be varied at will.

To determine a boundary layer profile the yawmeter was used in the following manner. The head was moved to the desired position on the wing surface, and, with the wind on, the yawmeter was adjusted until it just touched the wing surface. Readings were taken which enabled the static and dynamic pressures to be calculated at that point, and from the measured angle of outflow the velocity components along directions parallel and normal to the leading edge could also be determined.

Such readings were obtained over small increments of distance from the wing surface and the results are presented as boundary layer profiles in the two component directions.

Three series of readings were obtained as follows.-

- (i) At one position,  $\eta = 0.5$ ,  $x/c = 0.95$ ; for incidences  $0^\circ$ ,  $8^\circ$ ,  $10^\circ$ ,  $12^\circ$ . (see figs. 15 to 18).
- (ii) At one incidence,  $10^\circ$ ,  $\eta = 0.5$ ; for chordwise stations  $x/c = 0.3, 0.5, 0.7, 0.95$ . (see figs. 19 to 22).
- (iii) At one incidence,  $10^\circ$ ,  $x/c = 0.95$ ; for spanwise stations  $\eta = 0.15, 0.3, 0.5, 0.7$ . (see figs. 23 to 26).

### 3. Discussion

#### 3.1. The Tuft Explorations

On the whole, tufting was found to give a fairly reliable indication of the local directions of flow, although, at the surface, far more details are given by the use of the lampblack technique.

The method of reduction of the tuft results in this particular test produced a slight underestimate of the amount of outflow due to the fact that the tufts were glued onto pins and tended to lie along curves. The most useful and accurate parts of these curves occurred near the free end of the tuft, and in many cases this was unsteady.

The tufts could be relied upon to give the local flow directions with fair accuracy up to an incidence of approximately  $12^\circ$ , but at higher incidences the tufts became unsteady, particularly so near the tips. This region of disturbed flow extended inboards with increase in incidence. A similar effect has been observed<sup>(3)</sup> during some tests on a tapered wing with similar aspect ratio and sweepback but with a circular arc aerofoil section. In this case the onset of unsteadiness near the tips occurred at a slightly lower incidence.

Figs. 2 to 4 show the directions of flow over the unyawed wing. Consistent with the senses of the wing tip trailing vortices there was found to be a slight outflow on the lower surface at all distances from the surface. The amount of this outflow was found to have little variation with incidence over the range considered.

At distances greater than about a quarter of an inch from the upper surface there was a slight inflow. This was confirmed by the traverses with the yawmeter (see, for example, fig. 15). For smaller distances than  $1/4$ in. from the surface a strong outflow developed in the boundary layer towards the rear with the greatest deviations from the free stream direction occurring at the surface of the wing. This is to be expected since the adverse pressure gradient aft of the peak suction reduces the chordwise component of velocity by tending to produce a separation type of velocity profile in that direction, whilst the spanwise velocity profile is much less affected, consequently the flow adjacent to the wing is deflected through the largest angle.

The amount of outflow adjacent to the surface was in all cases found to increase towards the trailing edge. This outflow was found to develop near the root and to increase along the span; at low incidences this outflow appeared to reach a maximum at  $\eta = 0.75$ . Below an incidence of  $8^\circ$  the outflow was comparatively slight, but between  $8^\circ$  and  $12^\circ$  of incidence it developed rapidly until at  $12^\circ$  the direction of flow at the trailing edge was parallel to the trailing edge. All these effects are also clearly shown in the lampblack pictures in figs. 5, 6 and 7.

In figs. 2, 3 and 4 a spanwise flow off the tips is shown, particularly at the higher incidence. It would be expected that

/the flow ...

the flow would take up the free stream direction at a short distance outboard of the tip, but this area was not investigated fully.

The effect of yawing the model was found to increase the outflow on the backward moving wing, and to decrease it on the forward moving wing. This was equivalent to an increased and decreased angle of sweepback of the respective half wings. At  $10^\circ$  of yaw and an incidence of  $12^\circ$  the wing with increased sweepback developed a forward flow near the surface over the leading edge near the tip, and further increase in angle of yaw produced this type of flow at lower incidences. At  $20^\circ$  of yaw and  $12^\circ$  incidence this flow had become sufficiently thick for a tuft  $1/4$ in. from the surface to be affected.

### 3.2. The Lampblack Studies

The lampblack technique was found to be extremely useful in observing the flow adjacent to the wing surface. The technique was particularly informative in that it was possible to study the relative speeds of flow as the pattern developed. In analysing the flow characteristics shown by this method it must not be forgotten that the incidence of the wing was set before the tunnel was started. This was required because of the rapidity with which parts of the pattern were formed. It was thought, however, that no serious errors were introduced by this technique.

In the present series of tests the streamline indication of the directions of local flow agreed very well with the yawmeter measurements. However, the resulting patterns appear to differ in some measure from those produced by Black<sup>(1)</sup>, in that his results do not indicate the 'herring-bone' pattern found in these tests.

By observing the lampblack patterns during their formation it was seen that a fast flow near the surface left a pattern relatively clear of lampblack which shows up on the photograph as a lighter area (see, for example, fig. 7 near mid semispan towards the trailing edge). Conversely, dense concentrations of lampblack indicate very slow movement of the surface flow. This was found to take three distinct forms.-

- (1) a creeping flow along the leading edge of the upper surface (for example see fig. 5)
- (2) a 'herring-bone' pattern springing from the apex of the wing, suggesting a line of reattachment of the flow. (See fig. 9)
- (3) A standing vortex on the upper surface near the leading edge (a good example of this can be seen in fig. 9 near the mid semispan of the port wing).

Figs. 5 and 6 show the type of flow below  $10^\circ$  incidence, with uniform outflow developing towards the trailing edge, and with a creeping spanwise flow just after the leading edge. The flow at incidences of  $12^\circ$  and  $14^\circ$  (figs. 7 and 8 respectively) was similar to that at lower incidences, but over the rear half of the wing the flow collected into a fast outward moving stream which travelled forwards from the trailing edge and outwards towards the front of the wing tip. This indicates a region in which there has occurred separation of the turbulent boundary layer. This region has been labelled R in fig. 7. This region of separation has spread forwards and inward towards the root with increase of incidence to  $14^\circ$ .

At an incidence of  $16^\circ$  the nature of the pattern had changed suddenly, as shown in fig. 9. The simplified lower diagram has been lettered for ease of reference. Between A and B a marked dividing line was found in the form of a 'herring-bone' pattern. This is the line of reattachment after what is probably laminar separation at the leading edge. In front of this line the flow moved outwards to the leading edge, and collected as a standing vortex at F, in the region of peak suction (see reference 4). Behind AB the flow moved backwards and joined near C with the flow originating from the inboard trailing edge to move towards the tip at E. Here the flow divided, one section moving backwards and off at the tip, the other moving forwards and up at the leading edge to join the standing vortex at F.

At higher incidences the patterns were very similar, but with the increase in incidence, D has moved inboard, E has moved forward to the leading edge, indicating a further spread of the region of turbulent separation which occurred at  $\alpha = 12^\circ$ . The standing vortex at F has grown in both directions along the leading edge.

Figs. 10 and 13, call for special comment because the patterns were markedly anti-symmetrical. In both cases the standing vortex in the starboard wing had appeared to split into two. No explanation can be offered for this effect as it was very inconsistent. This would have been introduced as a critical incidence effect had it appeared only at  $16^\circ$  incidence, but it was also found at  $19^\circ$ . This pattern was produced in two runs out of five at  $16^\circ$  incidence, seeming to occur with no known change of conditions, and the effect could not be produced to order.

### 3.3. The Yawmeter Measurements

A limited number of these measurements were made to show the effects of incidence at one position on the surface, and to study the variations along the chord and span at an incidence of  $10^\circ$ .

Fig. 15 shows that the outflow develops rapidly after an incidence of about  $6^\circ$  is passed, the angle of outflow reaching  $61^\circ$  from the free stream direction at  $12^\circ$  incidence. Outside the boundary layer in the local free stream a slight inflow was noticed which increased with increase in incidence.

Fig. 16 shows the increase of boundary layer thickness with incidence, and at the same time the increased speed of flow just outside the boundary layer. In fig. 17 the chordwise boundary layer profiles are compared, showing that at zero incidence the  $1/7$ th power law was closely followed. With increase of incidence it is seen that the flow approached separation which finally occurred at an incidence just above  $10^\circ$ .

The spanwise distributions of velocity given in fig. 18 correspond closely to the  $1/7$ th power law at incidences below  $10^\circ$ . \* Outside the boundary layer the spanwise component of velocity,  $v$ , was about 0.68 of the undisturbed free stream velocity, which is consistent with a slight inflow superimposed on the spanwise component of  $U_\infty$ , which is  $1/\sqrt{2}$  or 0.707. At  $12^\circ$  of incidence, where the chordwise boundary layer profile clearly showed separation,  $v$  was nearly constant at  $0.6 U_\infty$  through about 80 per cent of the boundary layer thickness.

The remainder of the yawmeter measurements are presented in figs. 19 to 26. These show the variations over the surface at  $10^\circ$  incidence. This incidence was chosen as the incidence just prior to chordwise separation of the flow at 0.95 of the chord at mid semi-span.

The thickness of the boundary layer increased steadily across the chord reading 0.065c at 0.95 of the chord for the mid semi-span station. At 95 per cent of the chord the boundary layer thickness increased steadily on moving outwards from the root.

The chordwise component of velocity,  $u$ , just outside the boundary layer was found to decrease across the chord. This is associated with the adverse pressure gradient behind the peak suction. The isobar pattern for a similar wing<sup>(4)</sup> showed that the peak suction was close to the leading edge and extended over most of the semi-span. At 0.95 of the chord,  $u$  showed little variation outboard of  $\eta = 0.30$ , but decreased slightly near the root of the wing.

/Outside ...

---

\* This is consistent with the assumptions of Ref. 5.

Outside the boundary layer an inflow was found everywhere over the wing. At 95 per cent of the chord this inflow increased steadily along the semispan, reaching  $4^\circ$  at  $\eta = 0.70$ . At  $\eta = 0.50$  this inflow was found to decrease as the trailing edge was approached. From these values of inflow outside the boundary layer a nearly uniform rate of change of flow direction was noted per unit distance from the surface as the surface was approached, such that the outflow adjacent to the surface increased with the thickness of the boundary layer.

The chordwise boundary layer profiles deviated steadily from the  $1/7$ th power law near the leading edge of the wing to the verge of separation near the trailing edge due to the adverse pressure gradient across the chord. The tendency to separation was increased slightly near the tip, and appreciably decreased inboard of the position  $\eta = 0.30$ .

The spanwise components of velocity corresponded roughly to the  $1/7$ th power law over the leading three quarters of the chord, but some deviation was noticeable close to the trailing edge. Outside the boundary layer  $v$  varied between 0.67 and 0.70 of  $U_\infty$ .

#### 4. Conclusions

4.1. For incidences below  $8^\circ$  the outflow in the boundary layer was found to be small, but it developed rapidly between incidences of  $8^\circ$  and  $12^\circ$ . At  $12^\circ$  a region of turbulent separation formed at the trailing edge near the tip, and with increase in incidence this region spread forward and inwards towards the root. At  $16^\circ$  and above what appears to be laminar separation with reattachment occurred at the leading edge, and a standing vortex was formed.

4.2. At  $10^\circ$  of incidence an approximately constant rate of change of flow direction with distance from the surface was found through the boundary layer such that the angle of outflow at the wing surface was greater where the boundary layer was thickest.

4.3. The boundary layer thickness grew rapidly across the chord and also increased somewhat along the span, especially over the inboard half of the semispan. The boundary layer was thus thickest at the trailing edge near the tip.

4.4. Spanwise boundary layer profiles showed rough agreement with the  $1/7$ th power law, but showed a sudden departure as the angle of outflow approached  $45^\circ$ .

/4.5. ...

4.5. The effect of yawing corresponded to what one would expect for increased and decreased angles of sweepback on the rearward and forward moving half wings respectively. At large angles of yaw there was a region near the tip of the rearward moving wing in which a strong forward flow over the leading edge was observed.

-----  
REFERENCES

<u>No.</u>	<u>Author</u>	<u>Title, etc.</u>
1.	J. Black	Note on Vortex patterns in the boundary layer of a swept back wing. Jnl.Roy.Aero.Soc. Vol. 56, 1952, pp.279-285.
2.	G.G. Brebner	Pressure and Boundary Layer Measurements on a 59° sweptback wing at low speed. R.A.E. Report No. Aero. 2311a. A.R.C. C.P. No. 86.
3.	R.H. Neiley and W. Koven	Low Speed Characteristics in Pitch of a 42° sweptback wing with Aspect Ratio 3.9 and circular arc Airfoil Sections. N.A.C.A. R.M. L7E23 (1947).
4.	A.W. Babister	Measurement of the Pressure Distribution on sweptback wings with trailing edge split flaps. College of Aeronautics Report No. 43.
5.	A.D. Young and T.B. Booth	The Profile Drag of yawed wings of Infinite Span. College of Aeronautics Report No. 38.

APPENDIX

The Calibration and Use of a Conrad Yawmeter

If the yawmeter is yawed at an angle  $\theta$  from the direction of local velocity, pressures  $p_1$  and  $p_2$  will be recorded by the two tubes, and in general

$$p_1 = p + f_1(\theta) q$$

$$p_2 = p + f_2(\theta) q$$

where  $p$  and  $q$  represent the local values of static and dynamic pressures respectively. These pressures can be compared with free stream values (denoted by the suffix  $o$ ), and manometer readings can thus be presented as

$$R_1 = \frac{p_1 - p_o}{q_o}$$

and

$$R_2 = \frac{p_2 - p_o}{q_o}$$

In the calibration of the instrument measurements of  $R_1$  and  $R_2$  were obtained over a range of angles  $\theta$ . These results are plotted in fig. 27. It is seen that, over the range  $-15^\circ \leq \theta \leq 15^\circ$ , we may write

$$R_1 - R_2 = \frac{p_1 - p_o}{q_o} - \frac{p_2 - p_o}{q_o} = C_1 \cdot \theta \quad \dots\dots\dots (A.1)$$

$$R_1 + R_2 = \frac{p_1 - p_o}{q_o} + \frac{p_2 - p_o}{q_o} = 2.C_2 \quad \dots\dots\dots (A.2)$$

In a particular test the local direction of flow is first determined by rotating the yawmeter until  $R_1 = R_2$  and hence  $\theta = 0^\circ$ . The values of  $R_1$  and  $R_2$  are noted, and the yawmeter is then turned through  $10^\circ$ . Further values of  $R_1$  and  $R_2$  are recorded and equation A.1 gives

*redefined in the  $\frac{p_1 - p_o}{q_o}$  to  $\frac{p_1 - p}{q}$*

$$\frac{p_1 - p_o}{q_o} - \frac{p_2 - p_o}{q_o} = (R_1 - R_2)_{\theta=10^\circ} = \underbrace{\left( \frac{p_1 - p}{q} - \frac{p_2 - p}{q} \right)}_{w.c.1} \frac{q}{q_o} = 10.C_1 \cdot \frac{q}{q_o}$$

$$\therefore \frac{q}{q_o} = \frac{1}{10.C_1} (R_1 - R_2)_{\theta=10^\circ}$$

Also, equation A.2 gives

*$\frac{p_1 - p_o}{q_o} + \frac{p_2 - p_o}{q_o}$*

$$(R_1 + R_2)_{\theta=0^\circ} = \underbrace{\left( \frac{p_1 - p}{q} + \frac{p_2 - p}{q} \right)}_{2.C_2} \frac{q}{q_o} + 2 \cdot \frac{p - p_o}{q_o}$$

$$= 2.C_2 \cdot \frac{q}{q_o} + 2 \cdot \frac{p - p_o}{q_o}$$

/therefore ...

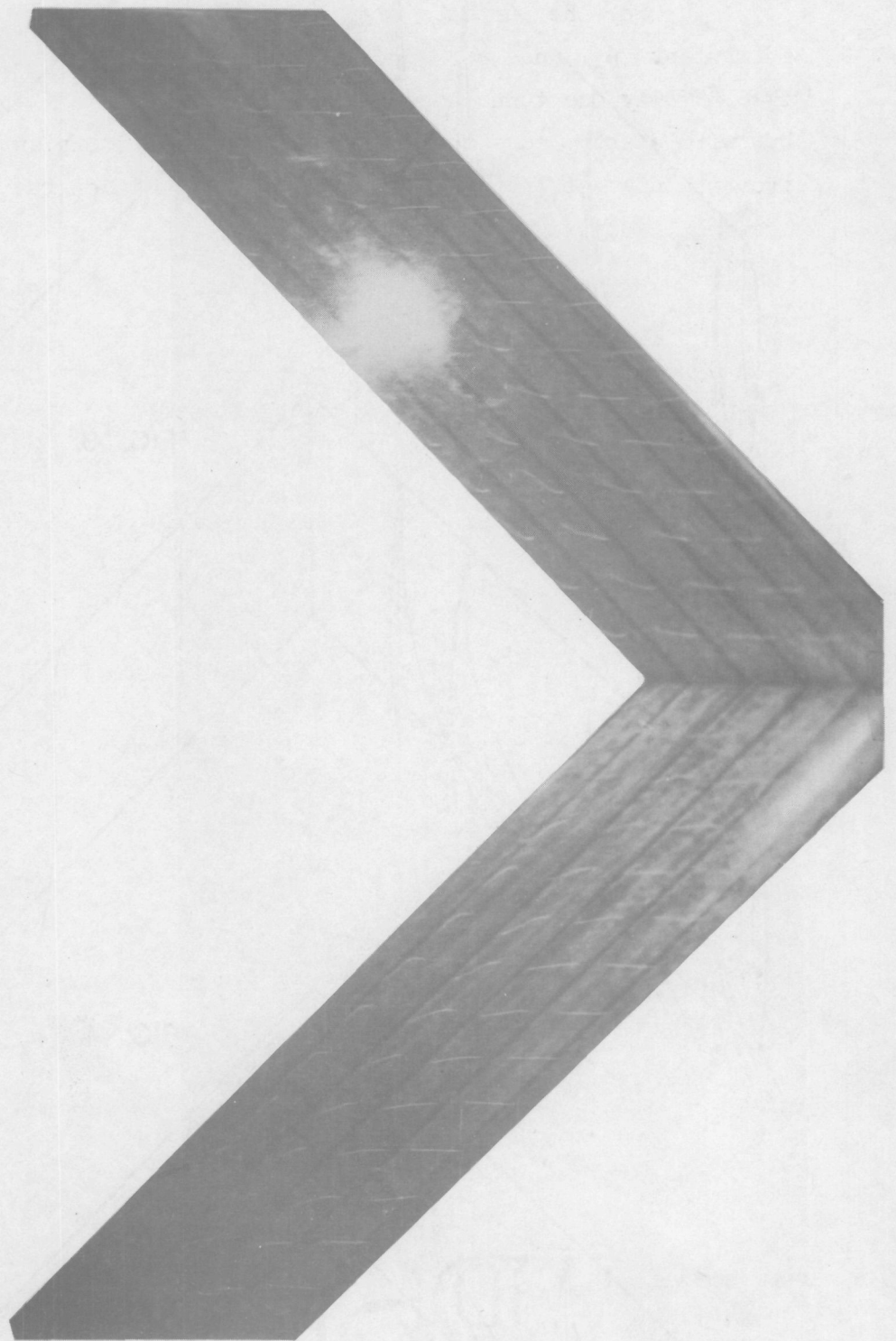
therefore 
$$\frac{p-p_0}{q_0} = \frac{1}{2} (R_1 + R_2)_{\theta=0^\circ} - C_2 \cdot \frac{q}{q_0}$$

For the purposes of the calibration of this particular instrument  $p_0$  and  $q_0$  were determined by a standard pitot static tube. Only one tunnel speed was considered, namely 130 ft./sec., but with a sharp edge to promote permanent or incipient breakaway from the nose of the yawmeter any scale effects on the calibration are not likely to be serious.

The effect of pitch has also been investigated and was found to be very small. An error of  $10^\circ$  in pitch led to a 3 per cent error in dynamic pressure. Brebner<sup>(2)</sup> found that  $6^\circ$  error in pitch caused a 1 per cent error in this quantity.

----

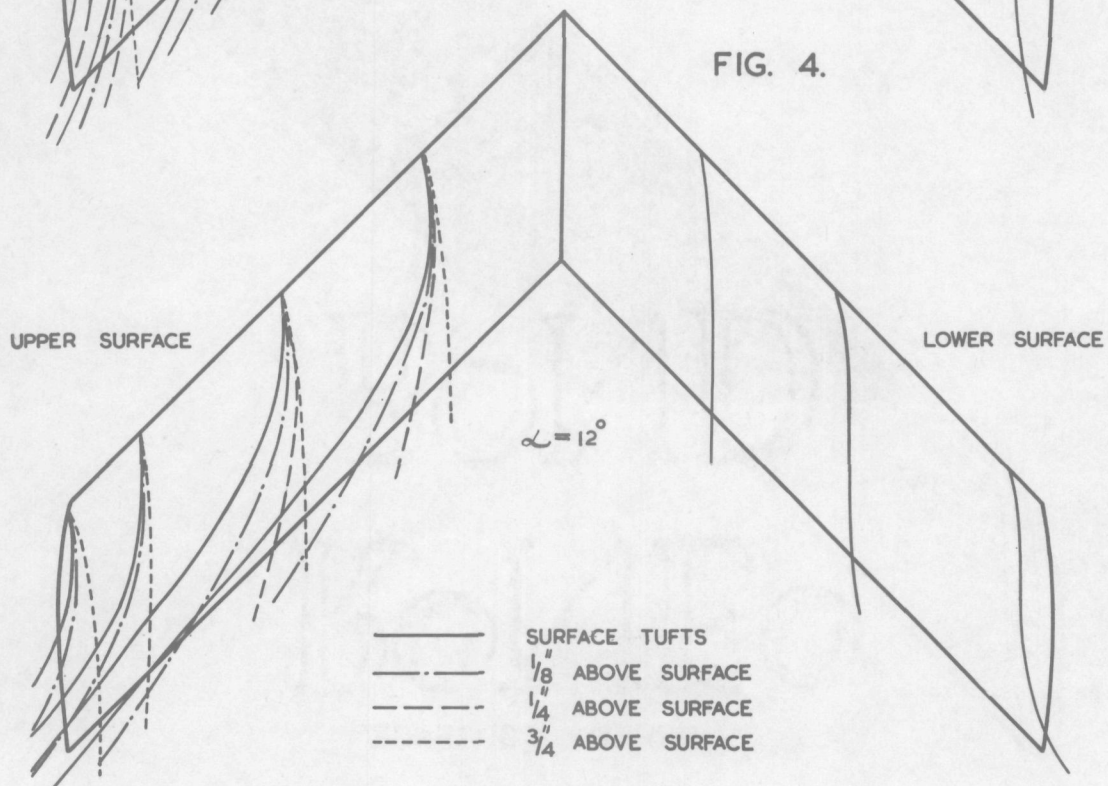
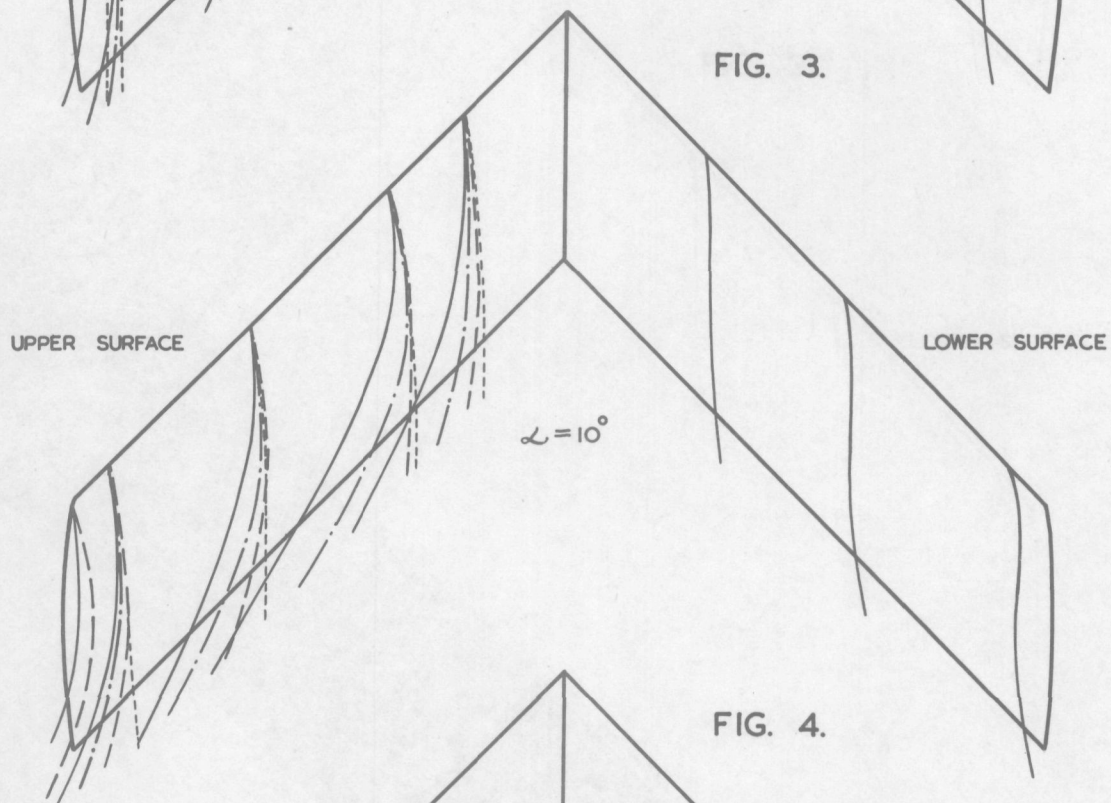
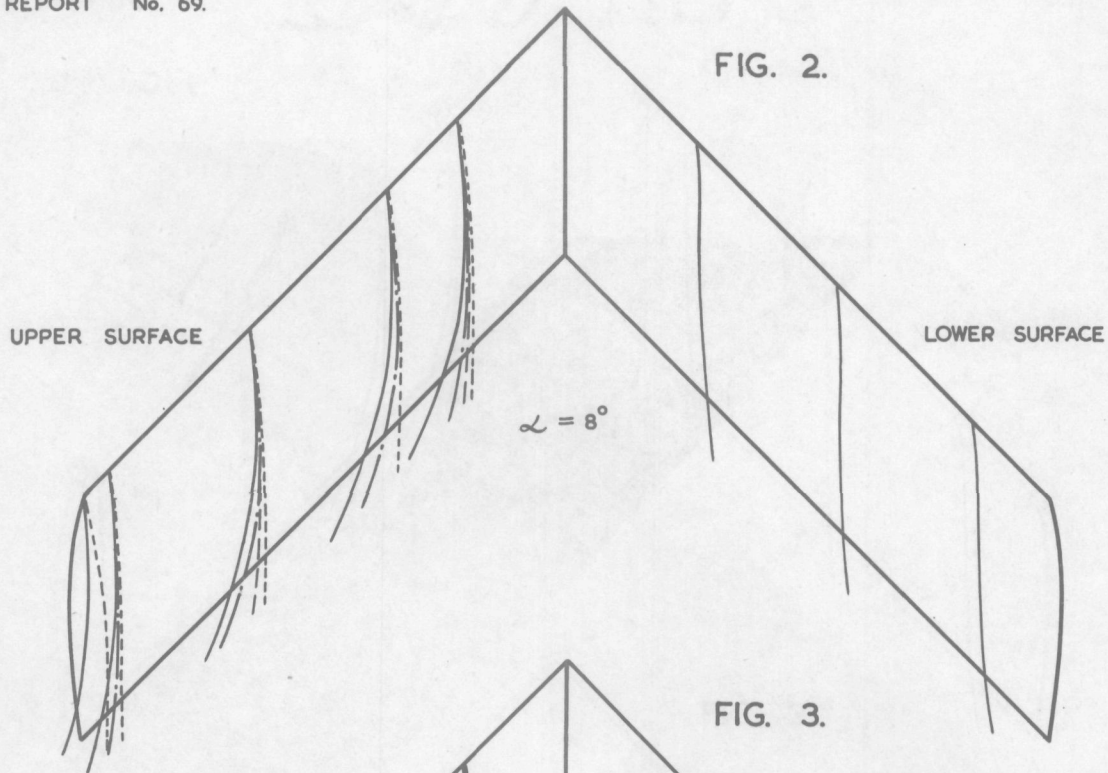
FIG. 1.

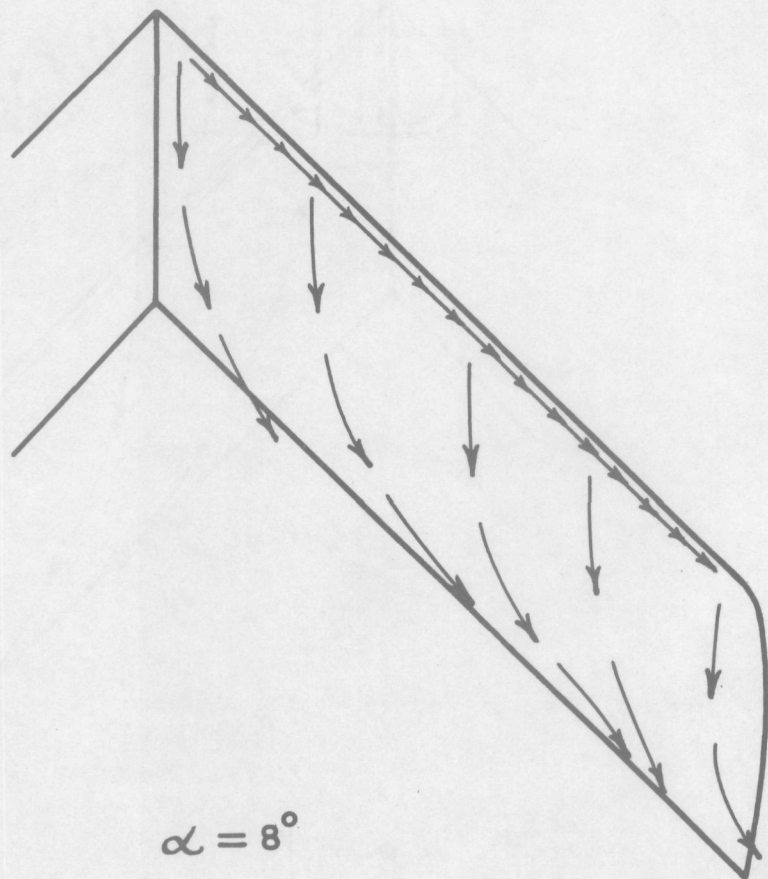
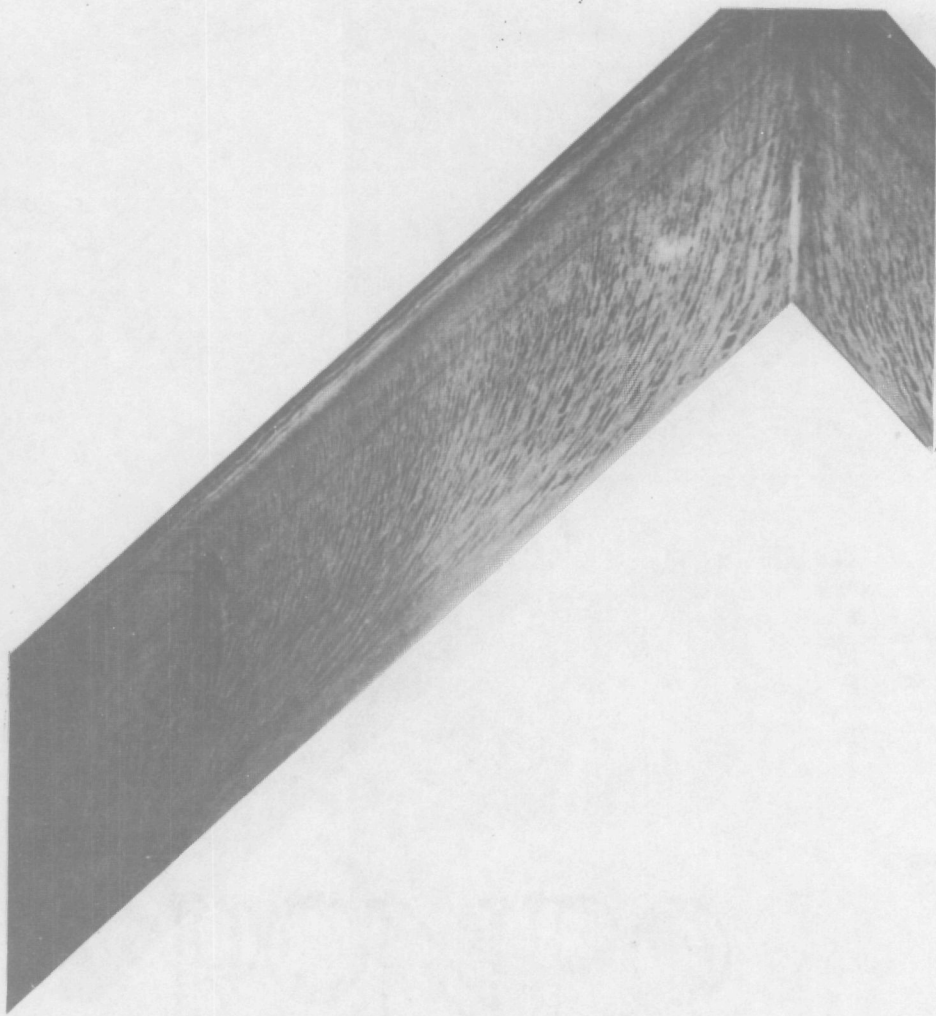


UPPER SURFACE

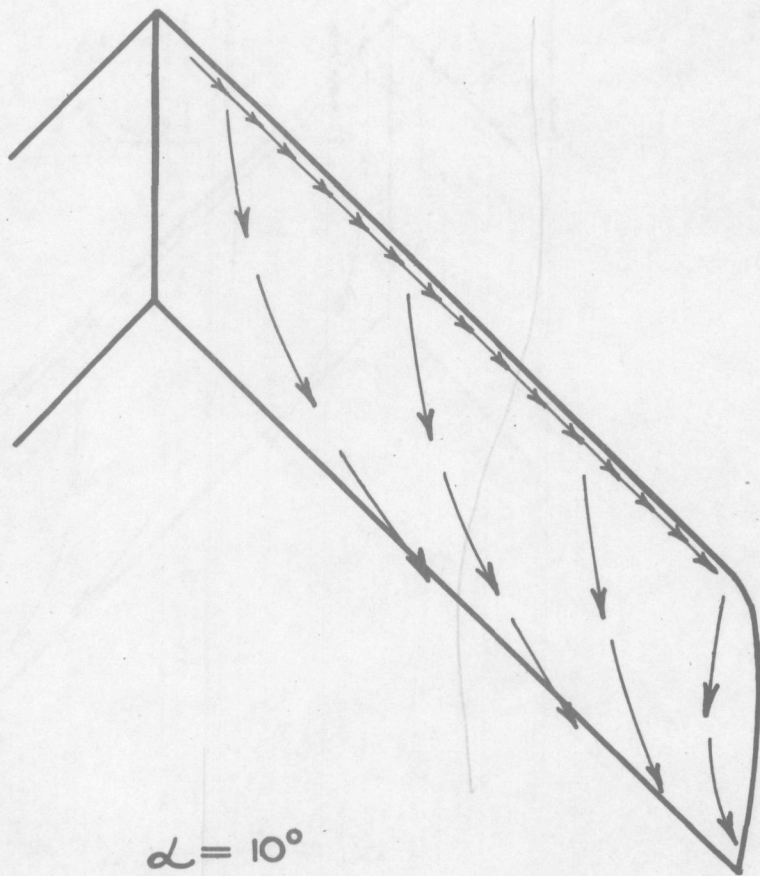
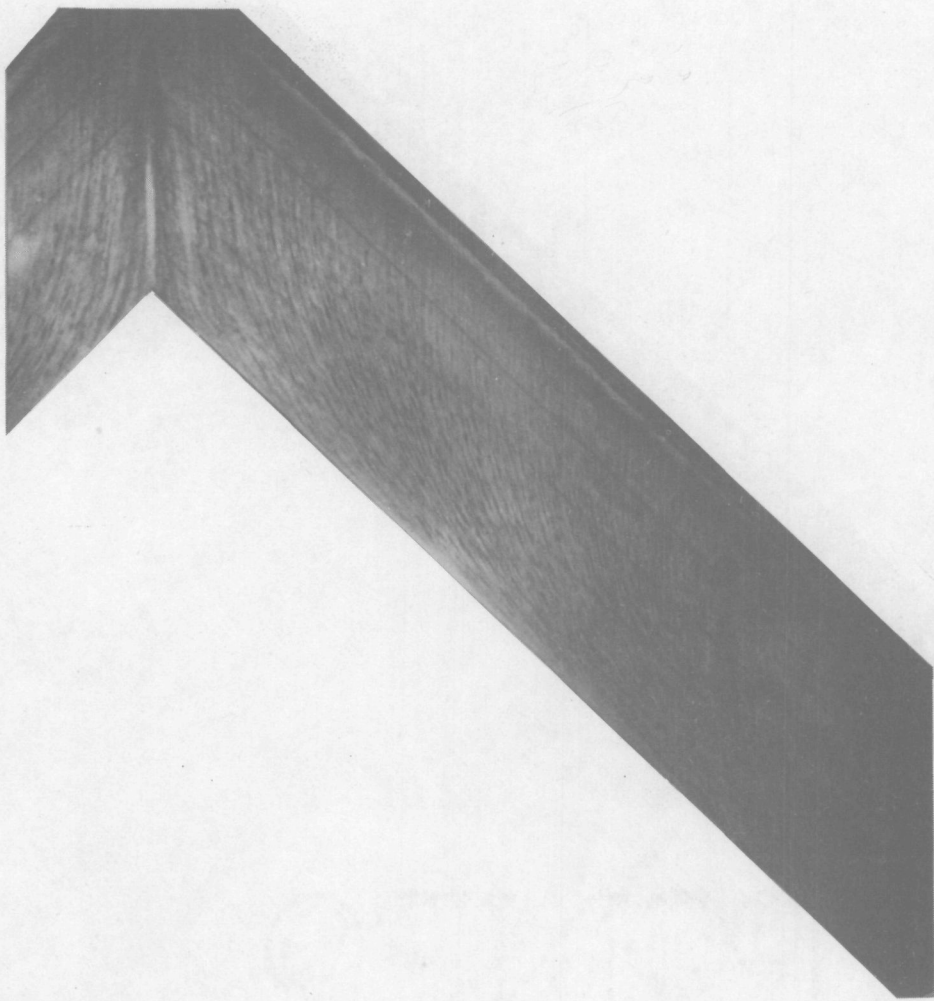
$$\alpha = 10^\circ$$

SURFACE TUFT PICTURE



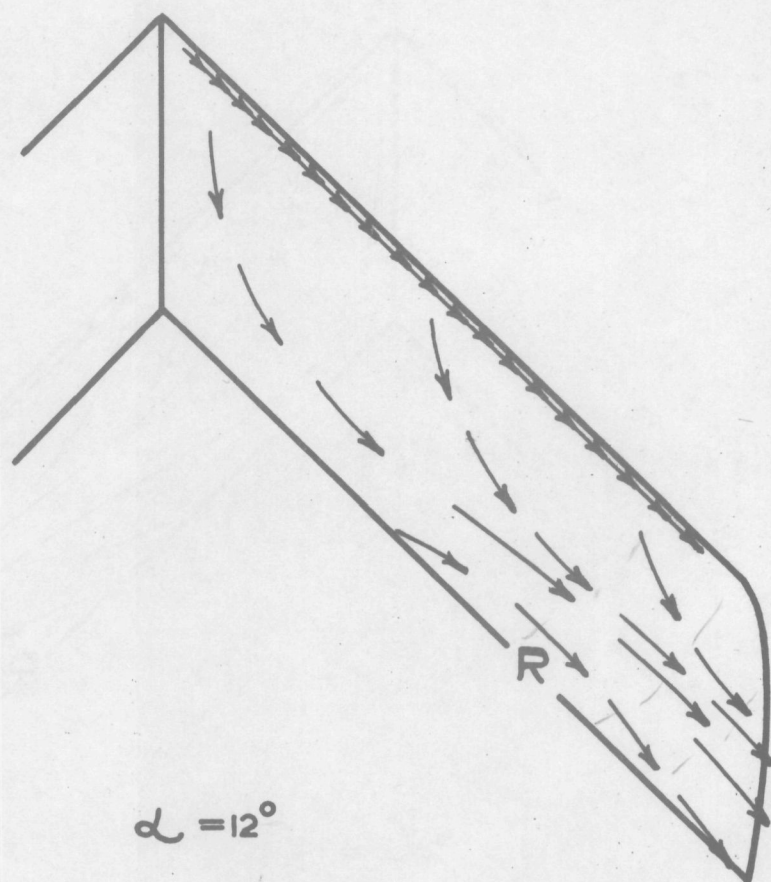
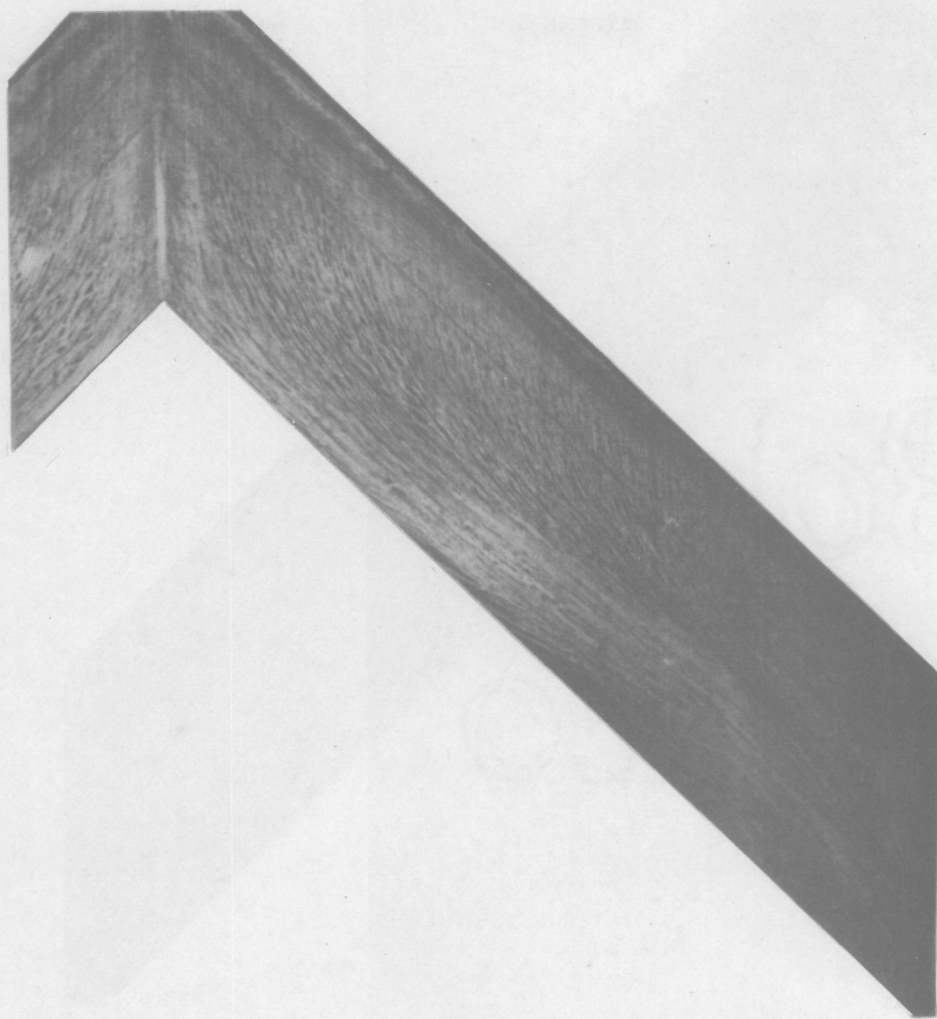


LAMPBLACK PATTERN ON UPPER SURFACE

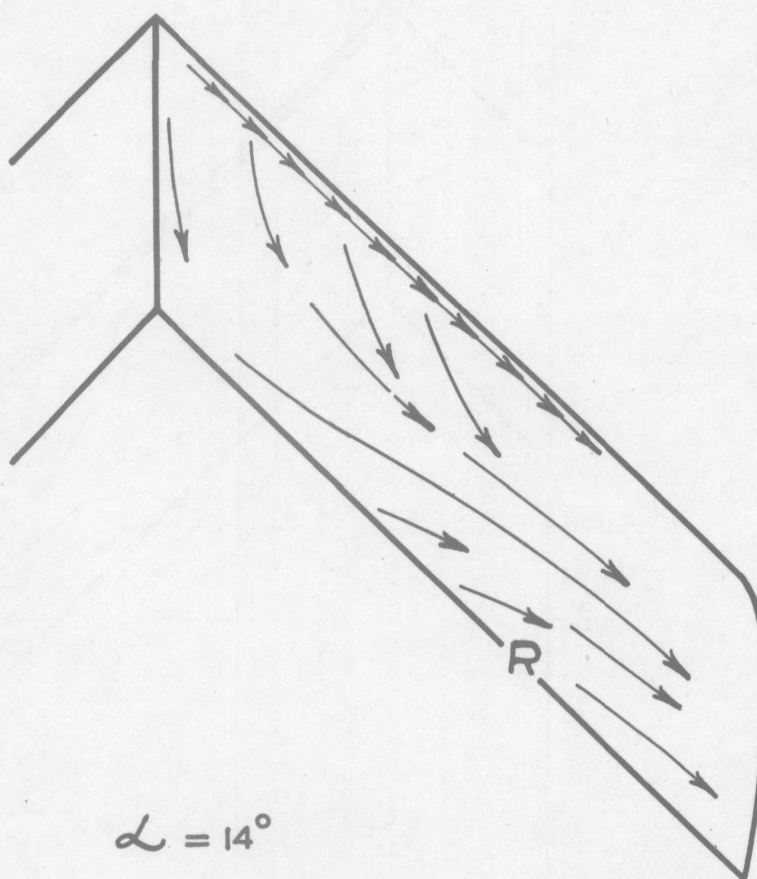
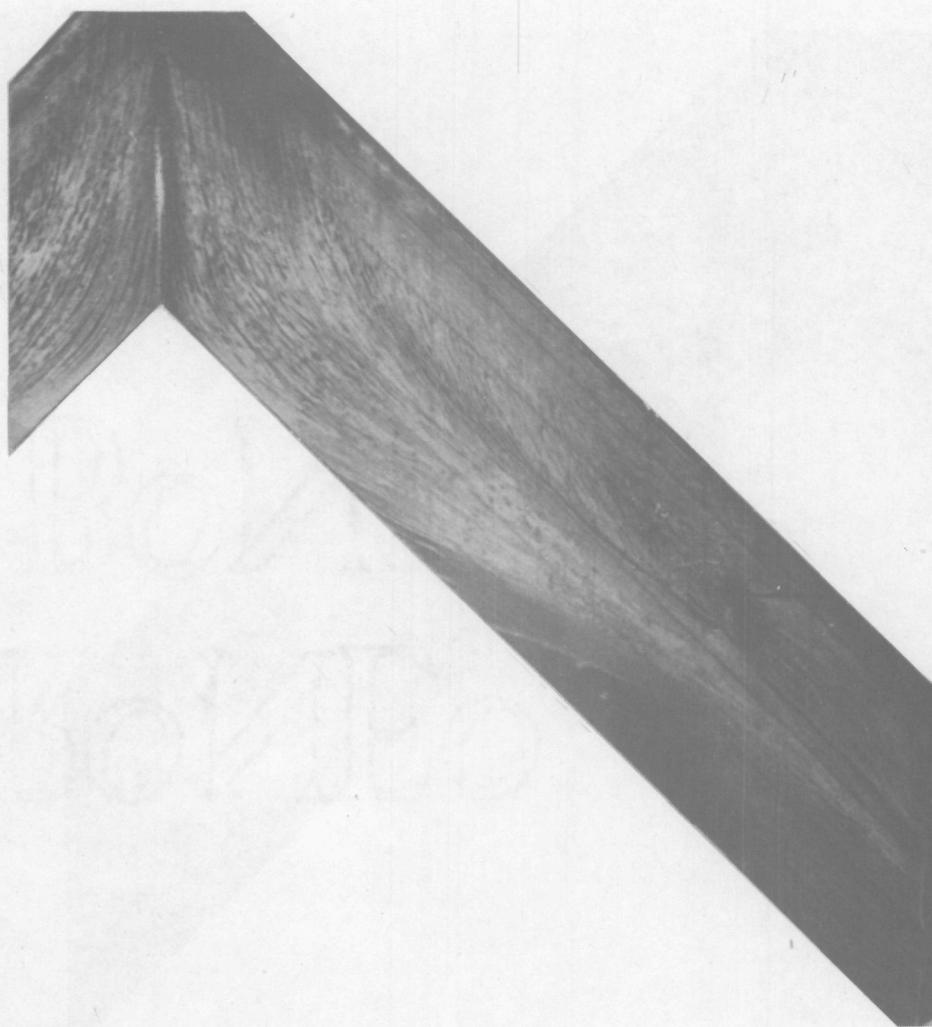


$$\alpha = 10^\circ$$

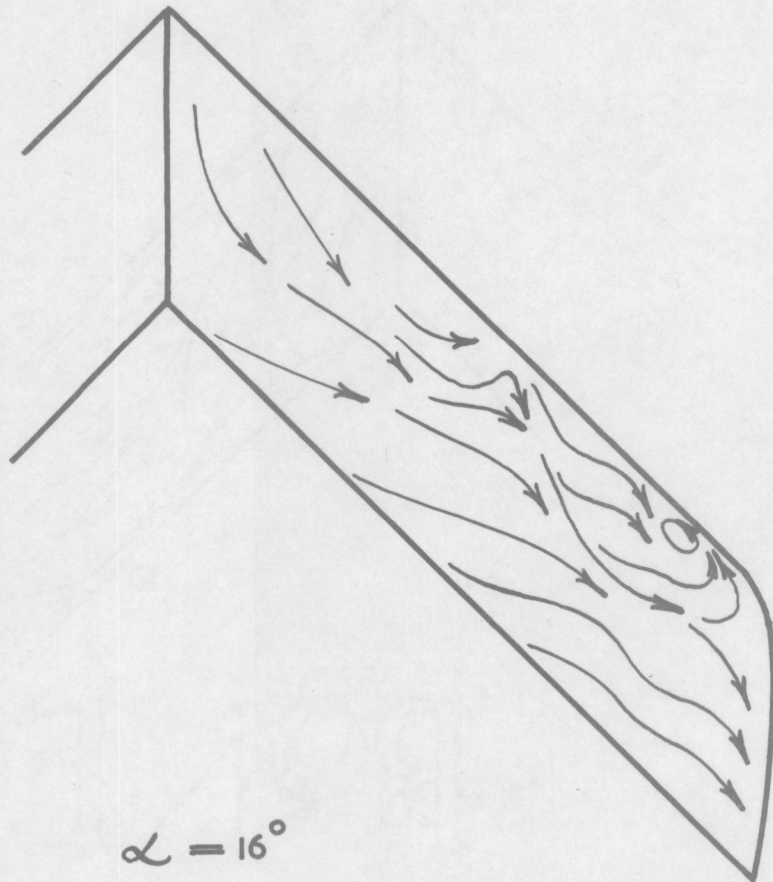
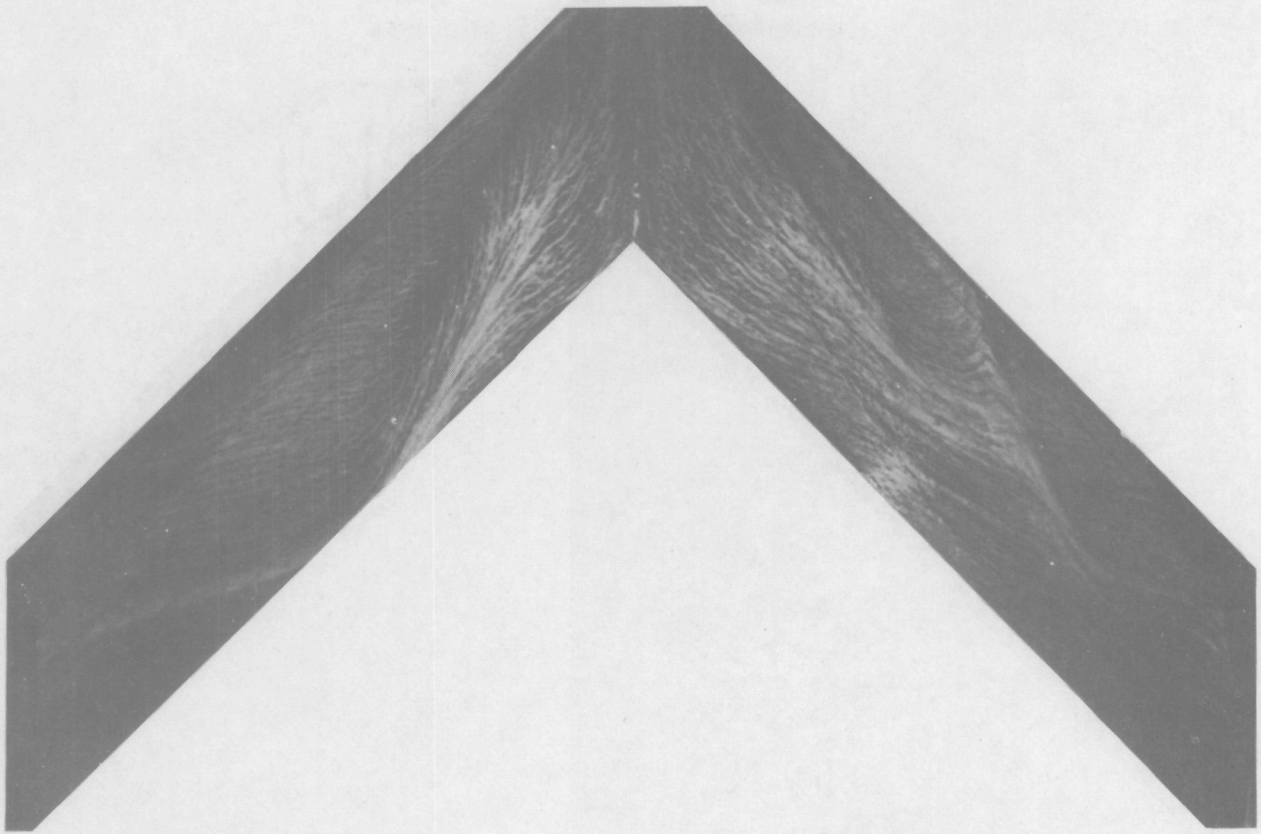
LAMPBLACK PATTERN ON UPPER SURFACE.



LAMPBLACK PATTERN ON UPPER SURFACE.

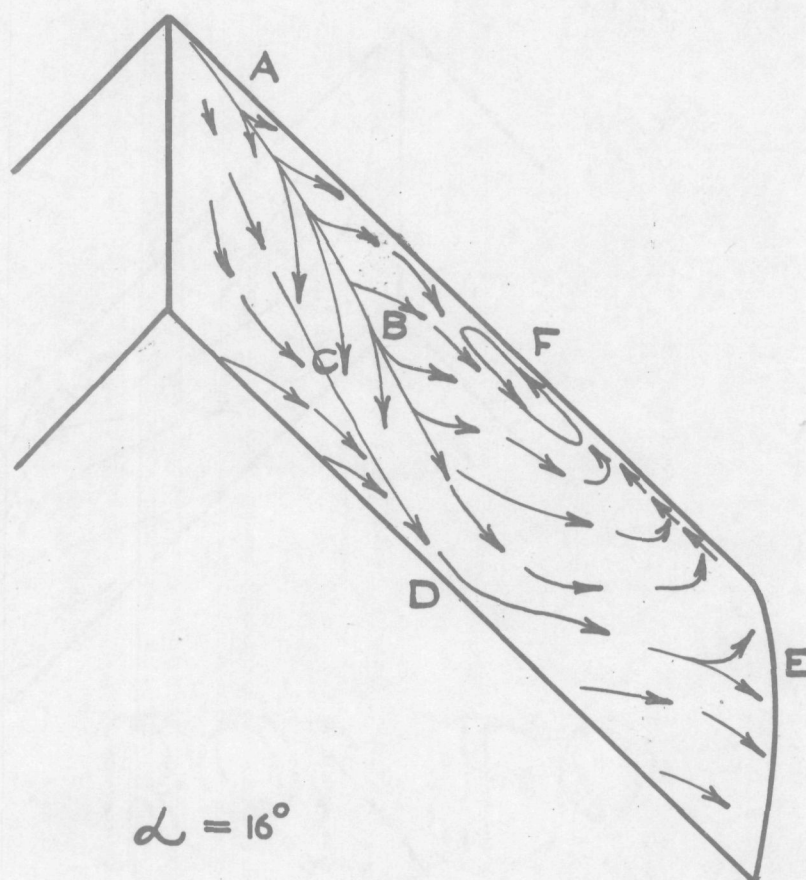
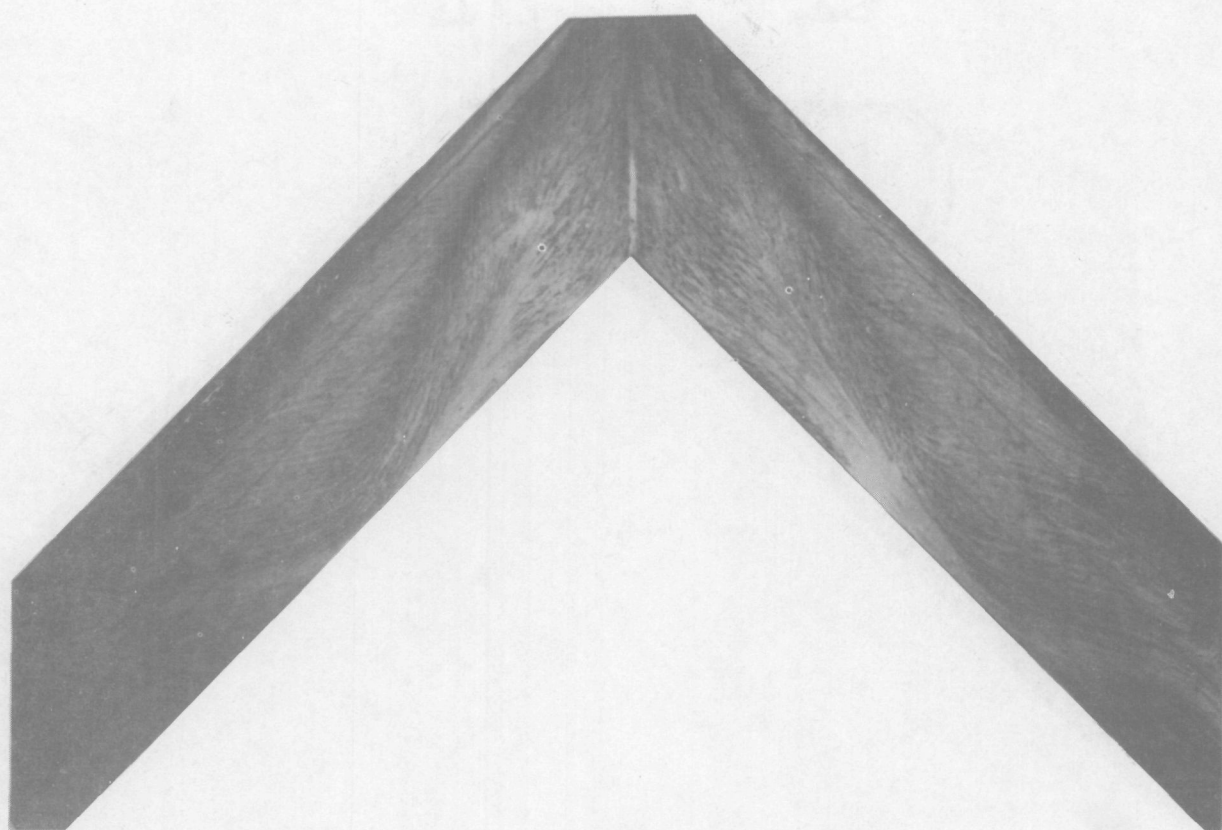


LAMPBLACK PATTERN ON UPPER SURFACE.

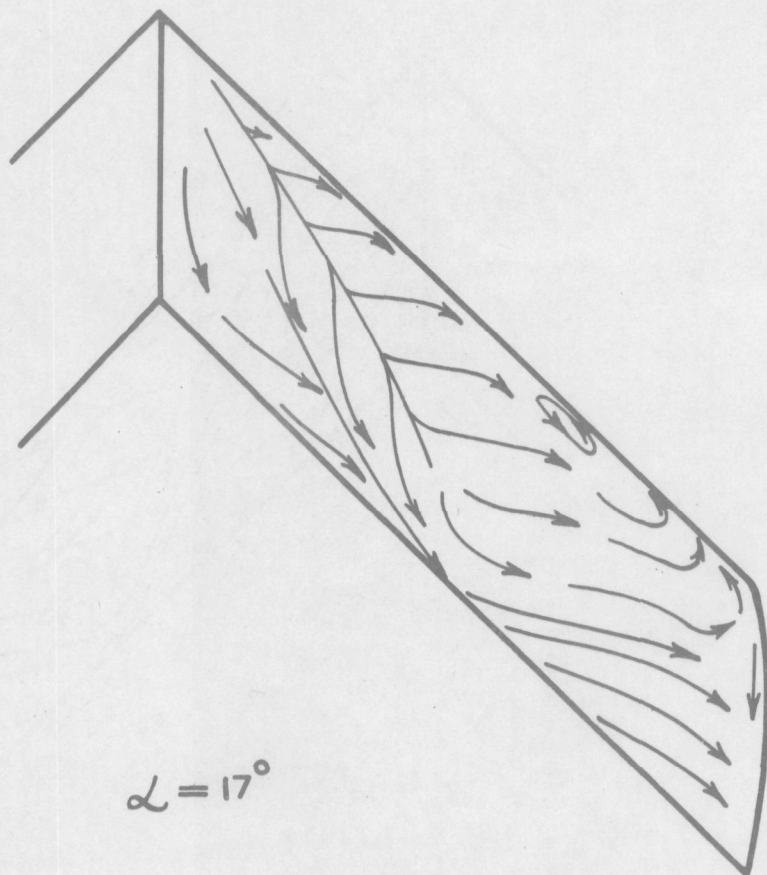
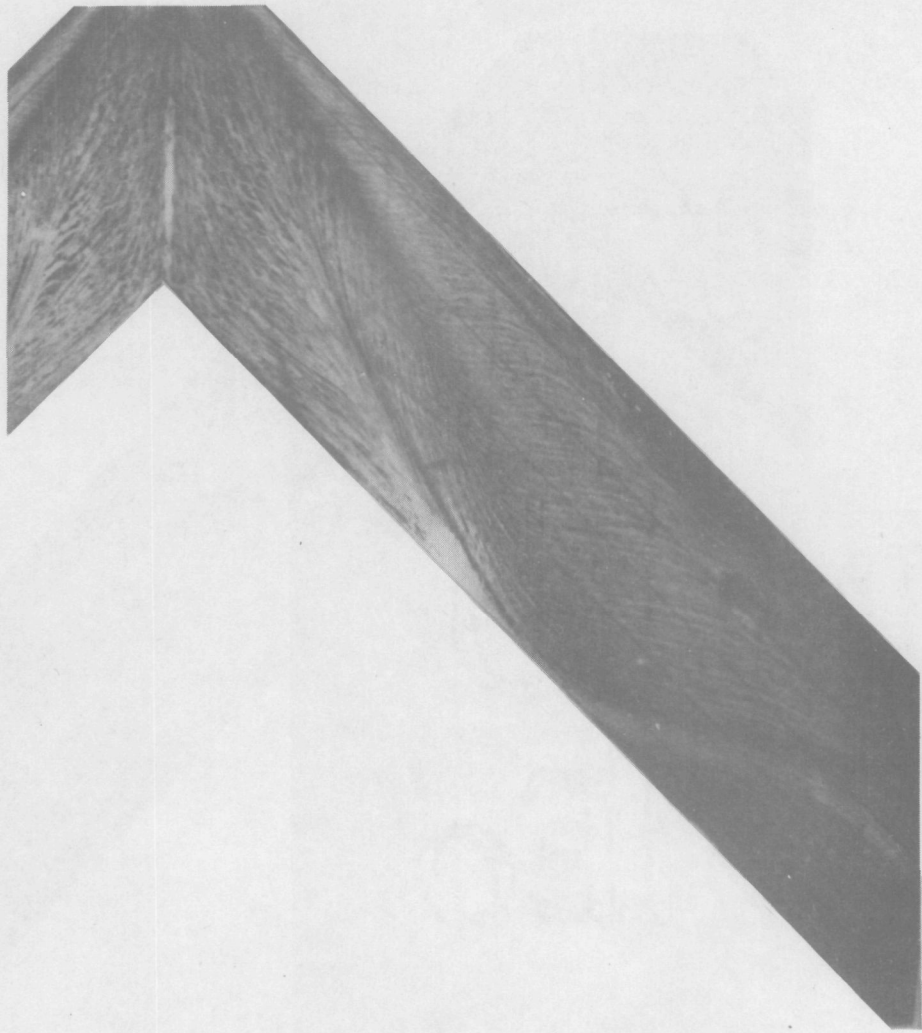


$$\alpha = 16^\circ$$

LAMPBLACK PATTERN ON UPPER SURFACE.

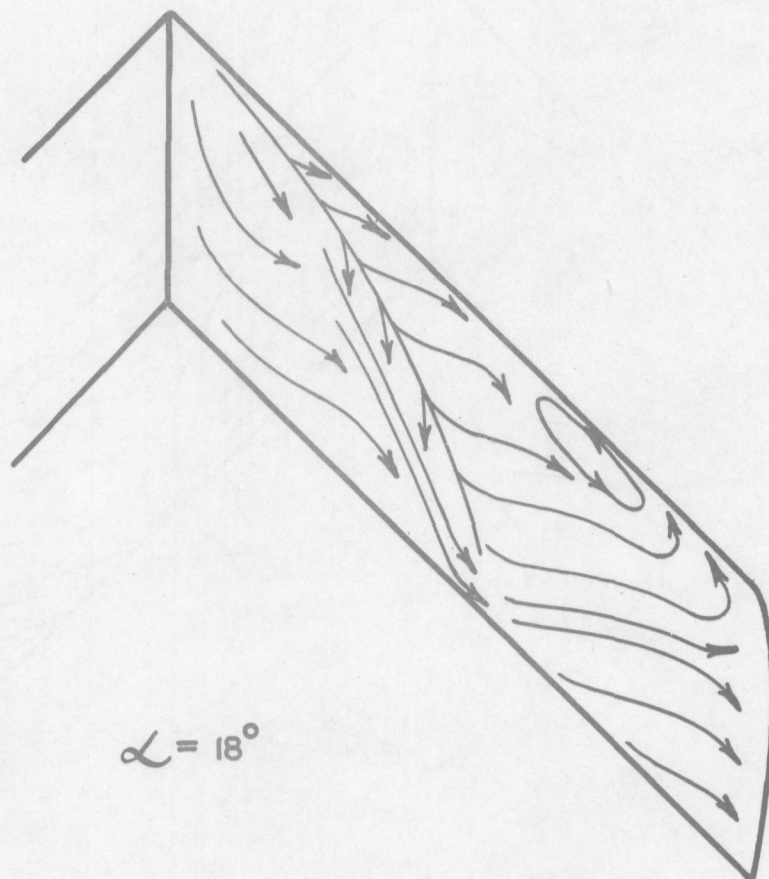
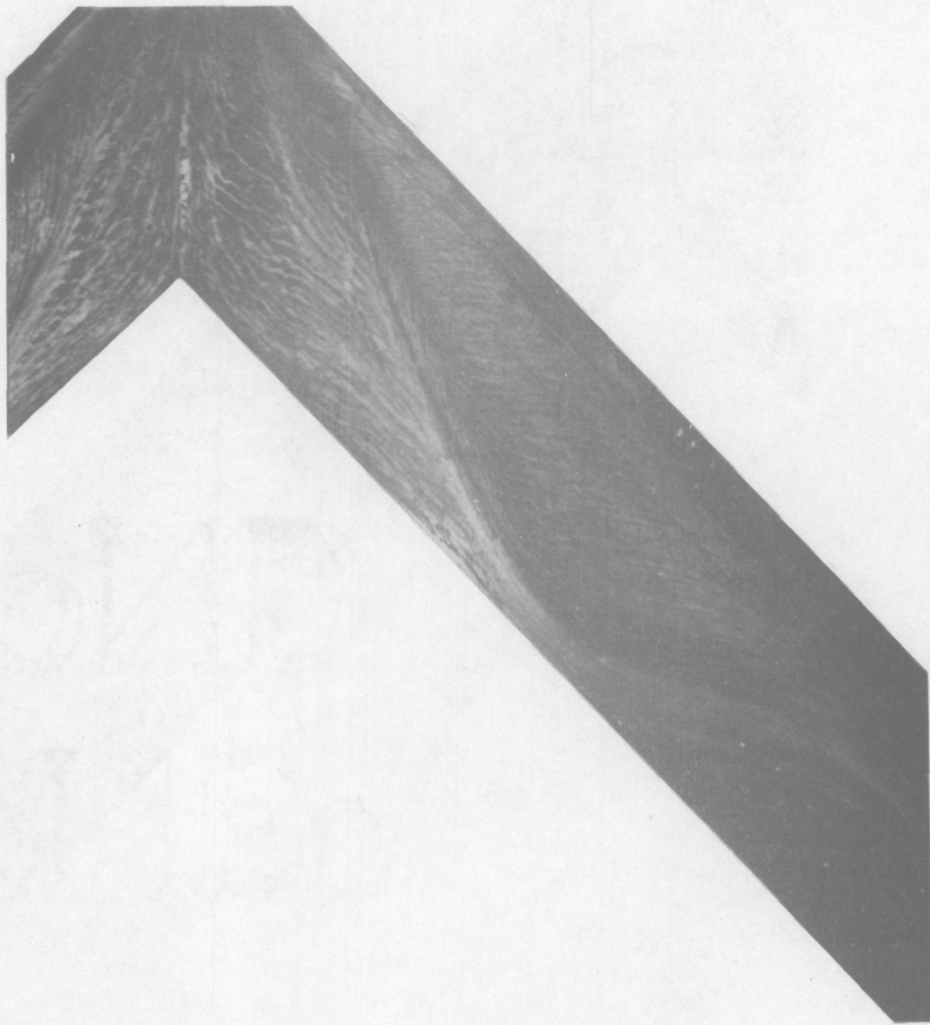


LAMPBLACK PATTERN ON UPPER SURFACE.

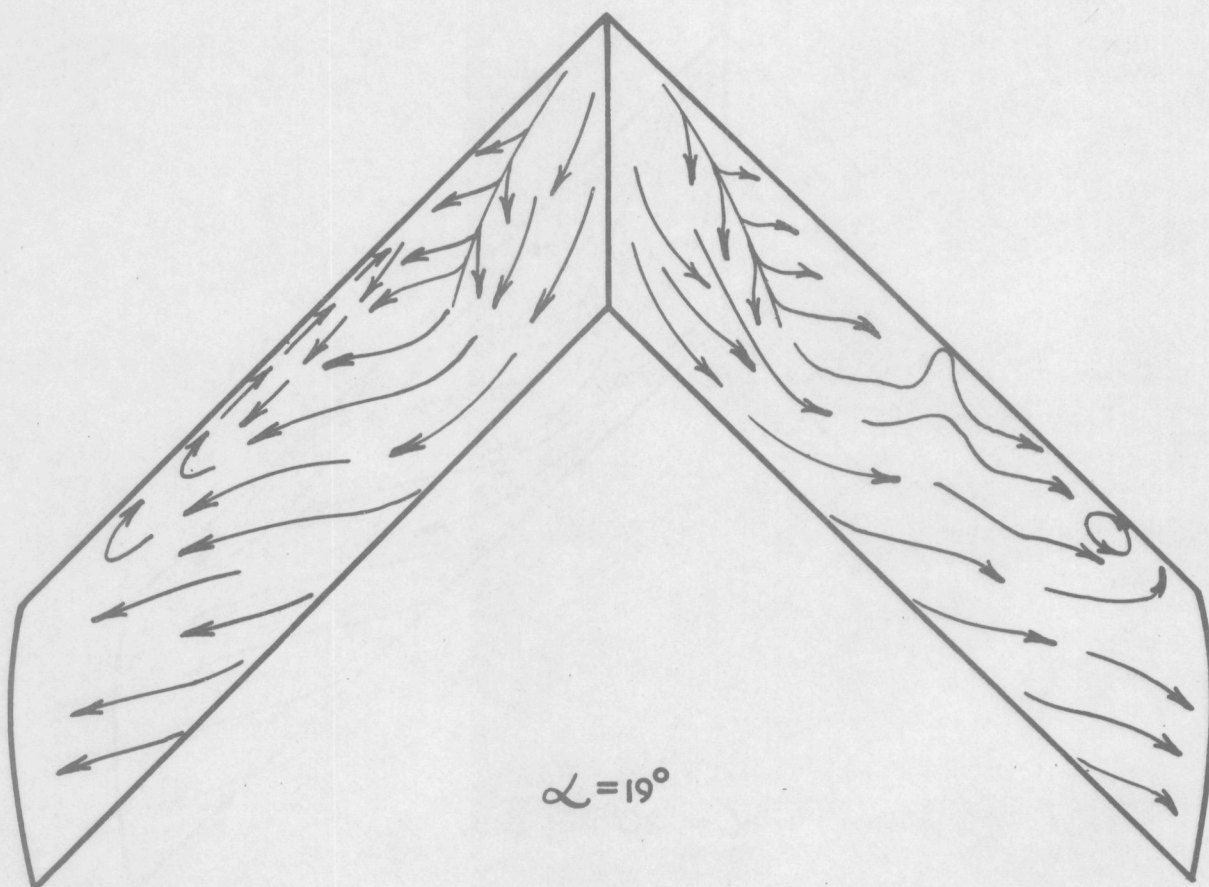
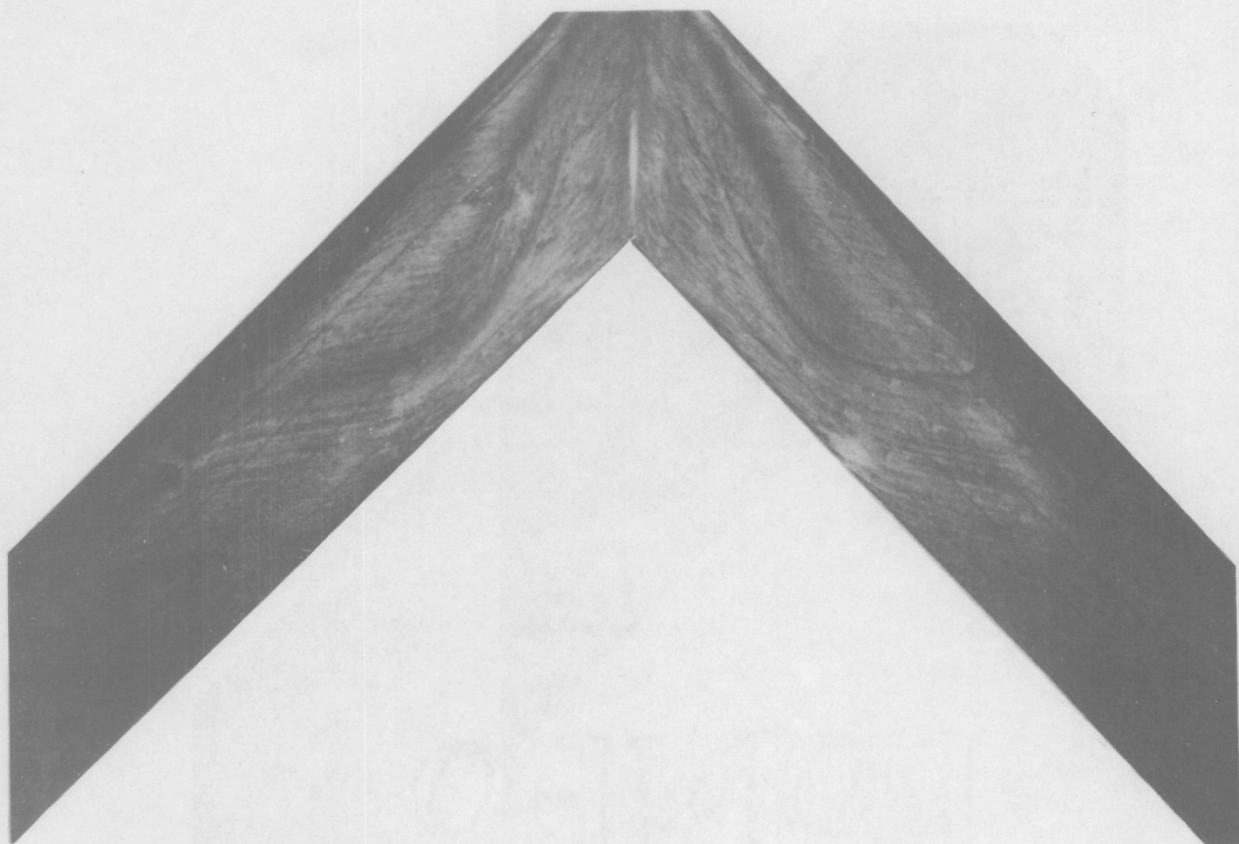


LAMPBLACK PATTERN ON UPPER SURFACE.

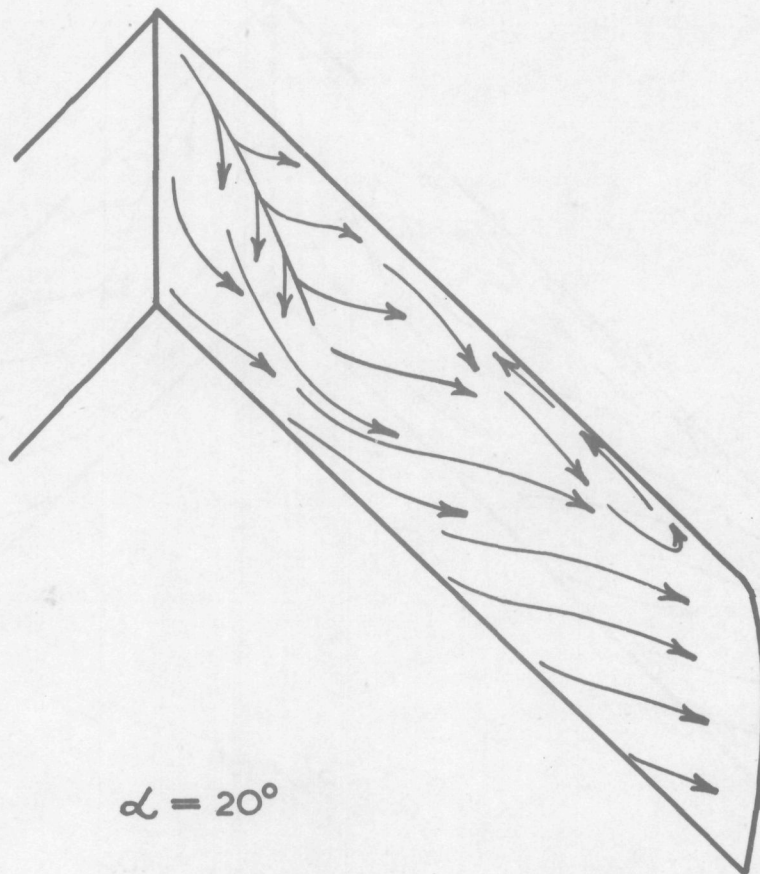
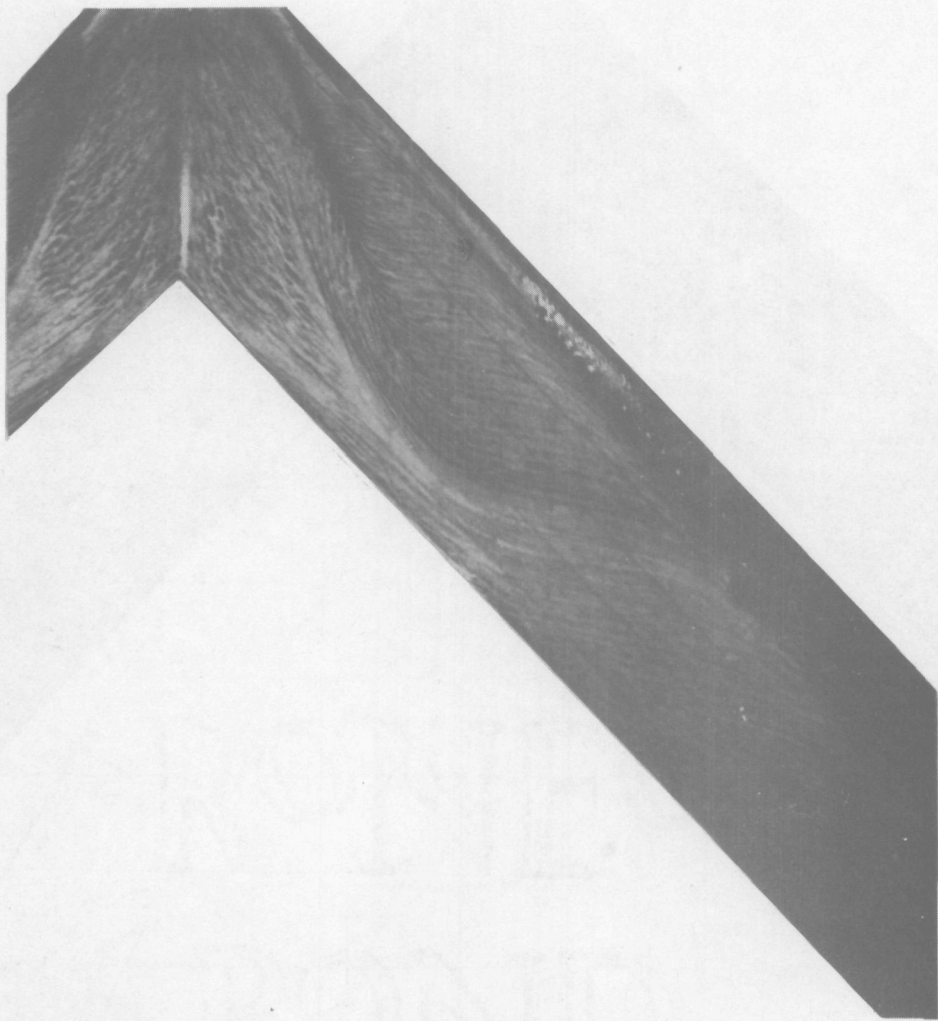
FIG. 12.



LAMPBLACK PATTERN ON UPPER SURFACE.

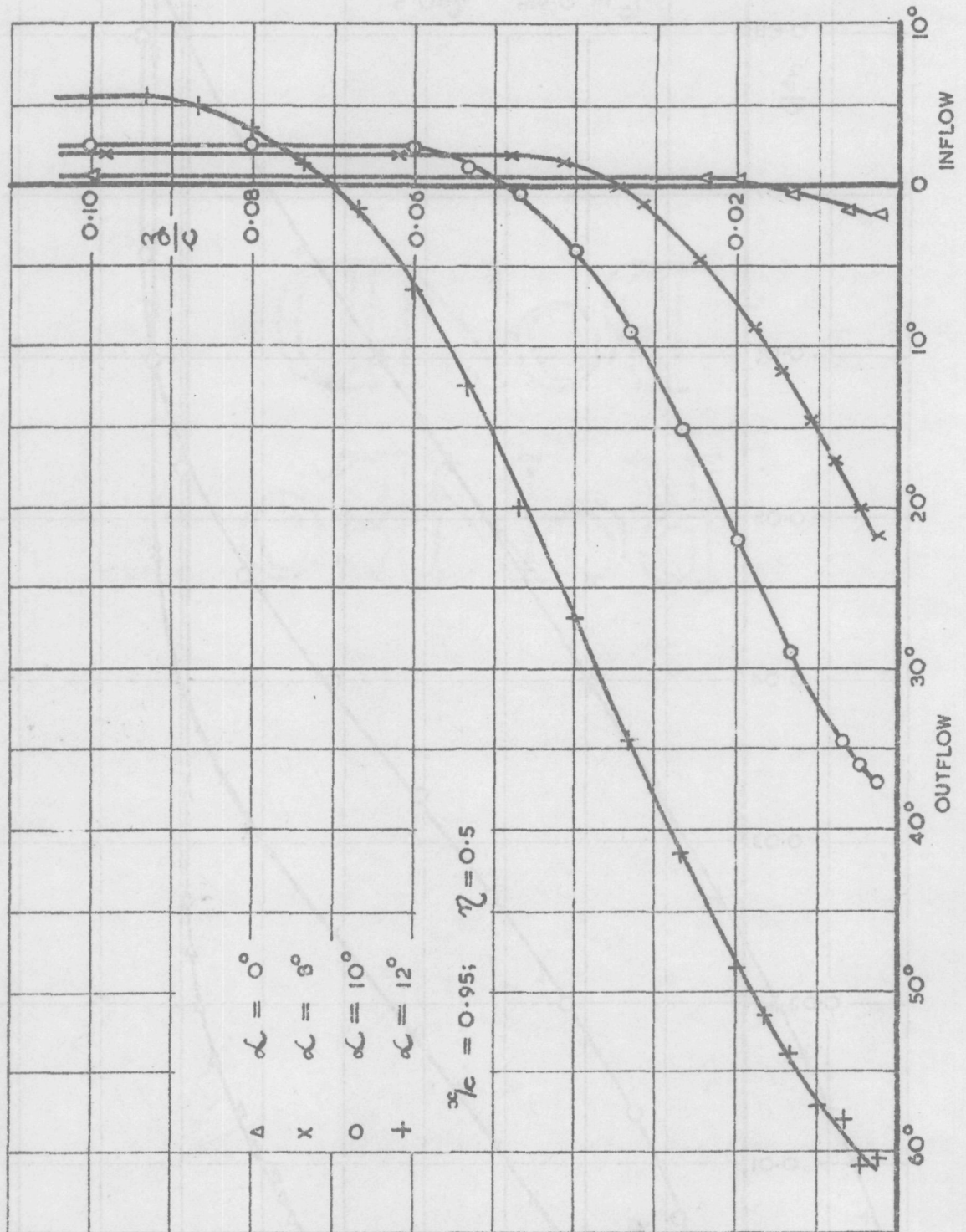


LAMPBLACK PATTERN ON UPPER SURFACE.



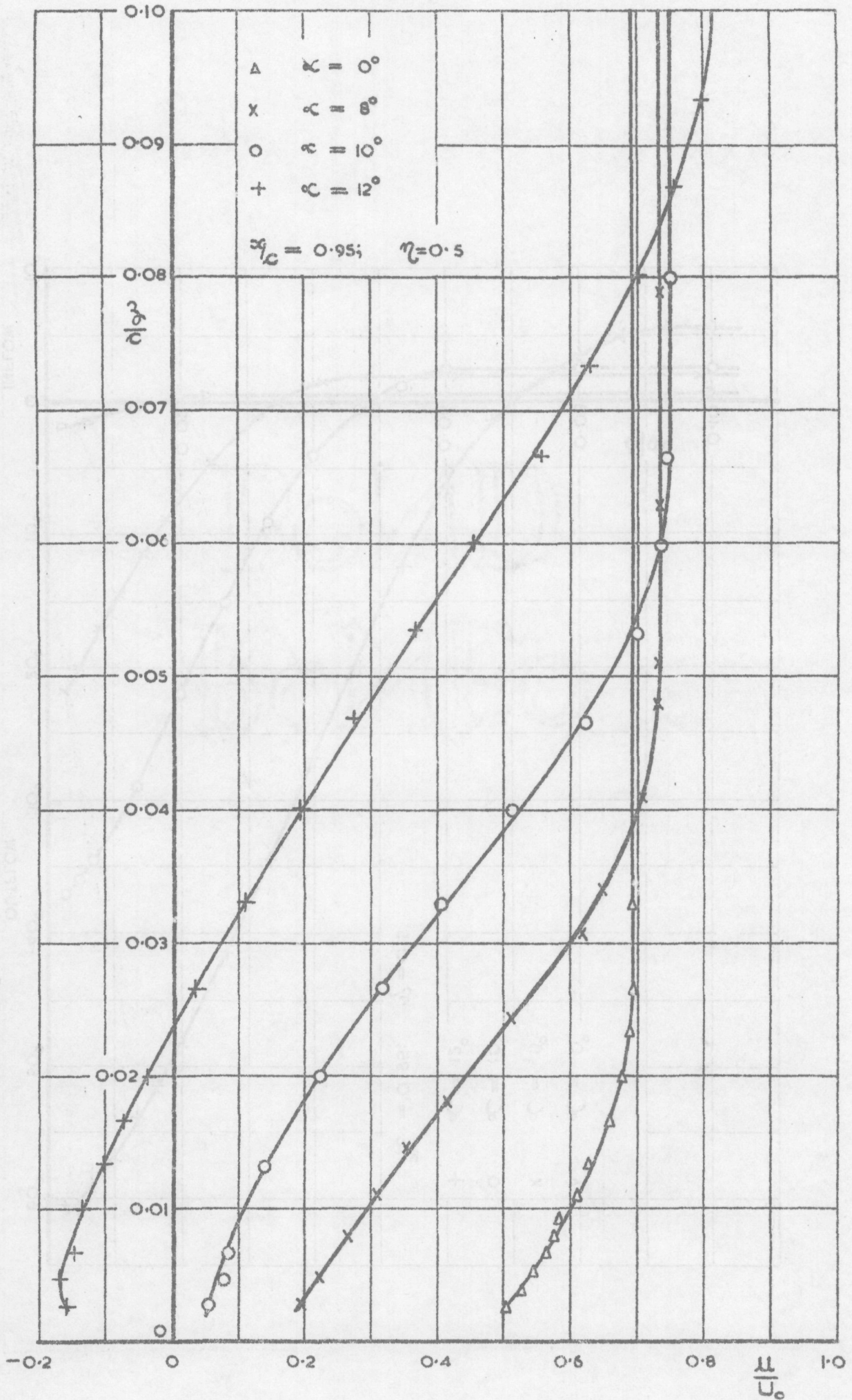
$$\alpha = 20^\circ$$

LAMPBLACK PATTERN ON UPPER SURFACE.

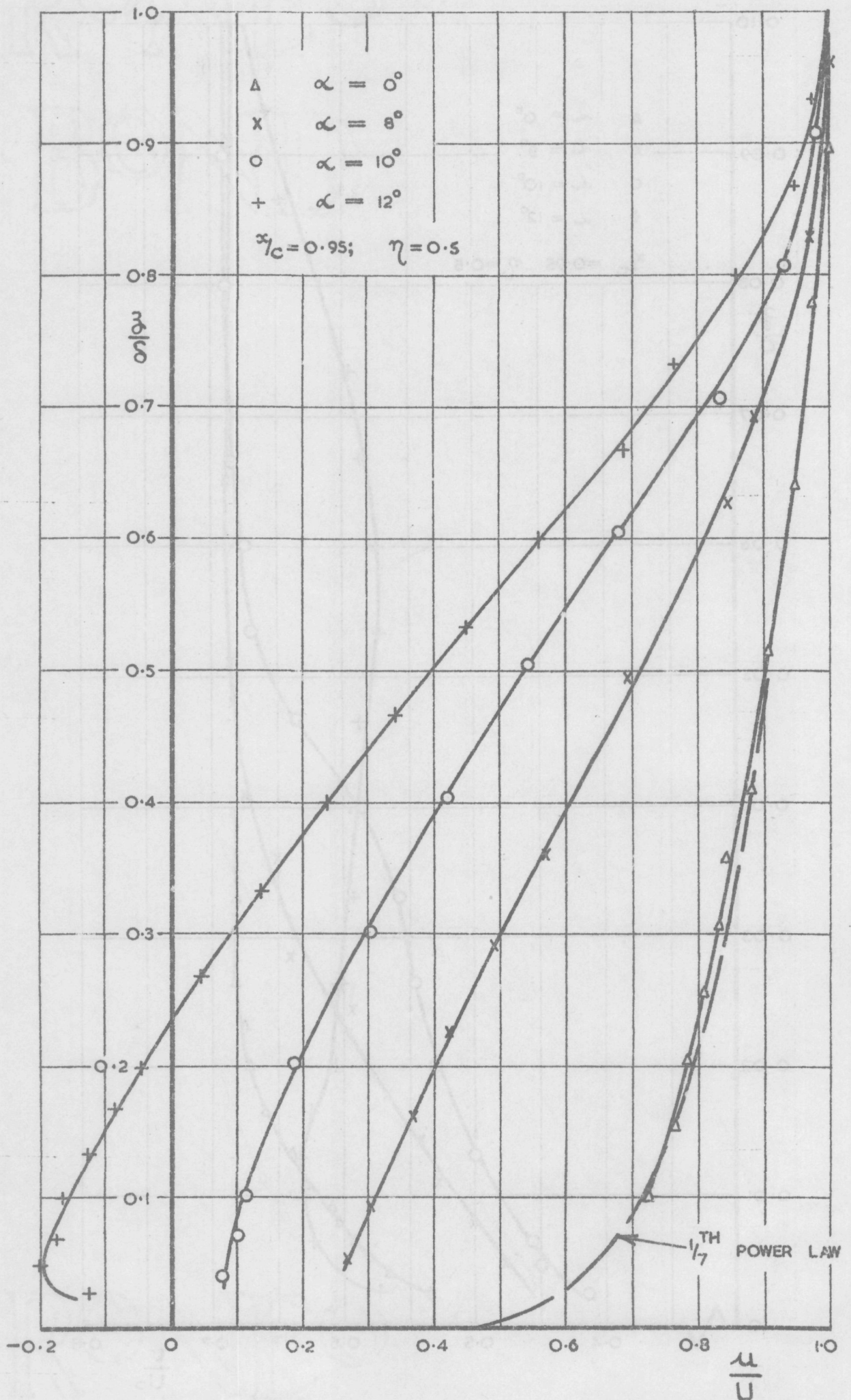


ANGLES OF FLOW THROUGH BOUNDARY LAYER.  
 VARIATION WITH INCIDENCE.

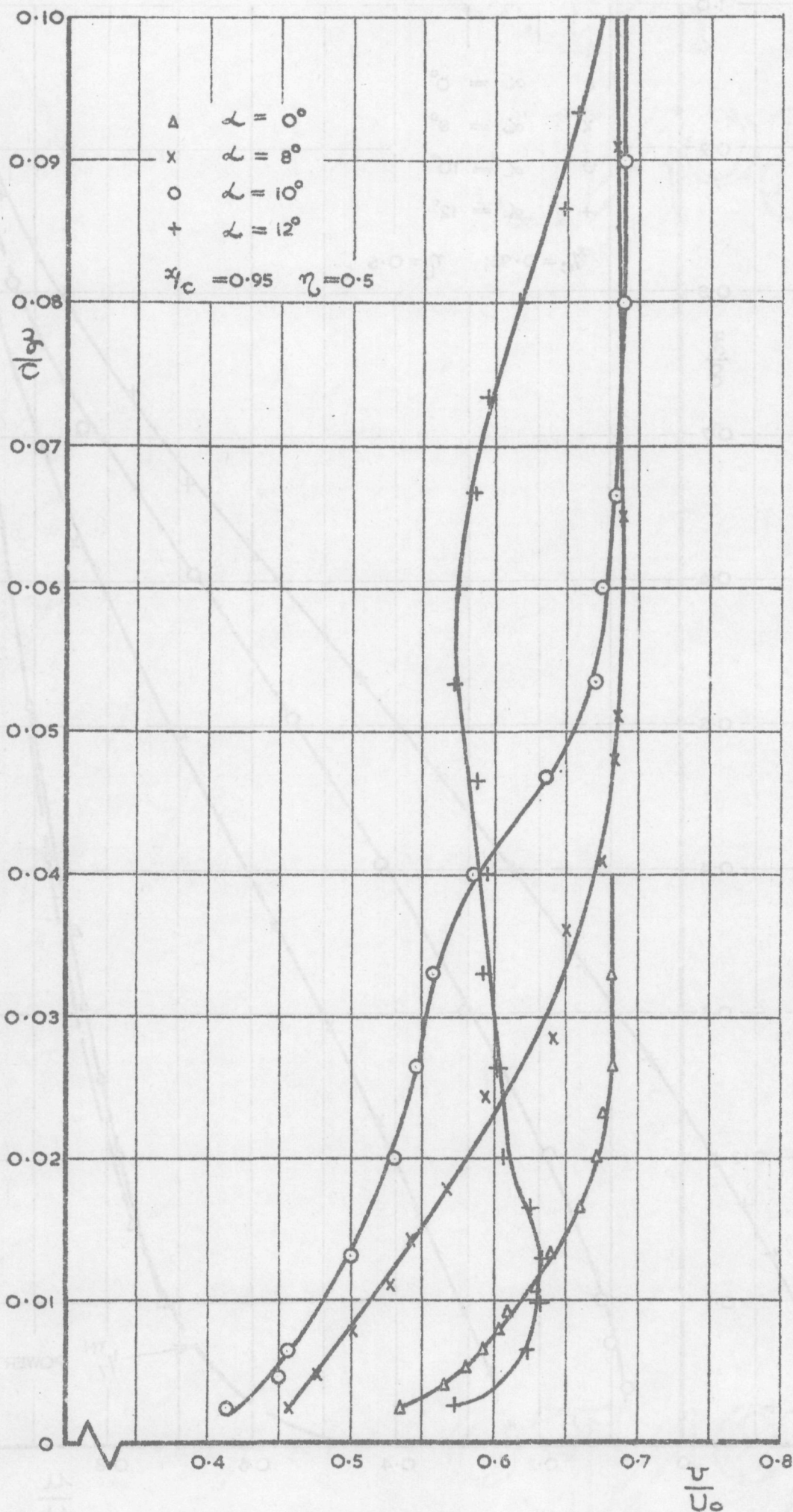
FIG. 16.



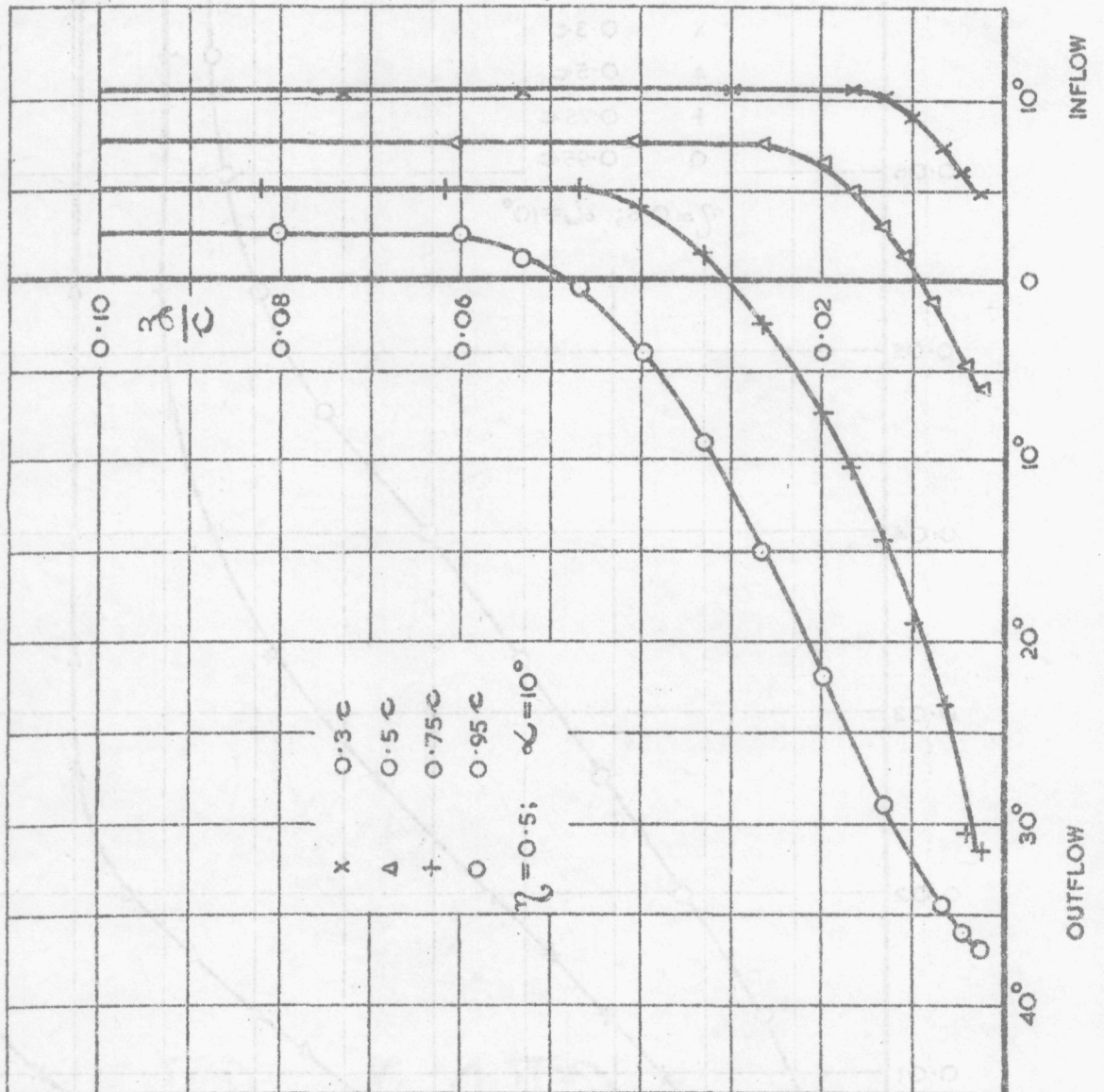
CHORDWISE VELOCITY DISTRIBUTION THROUGH BOUNDARY LAYER.  
 VARIATION WITH INCIDENCE.



CHORDWISE BOUNDARY LAYER PROFILE. VARIATION WITH  
 INCIDENCE.

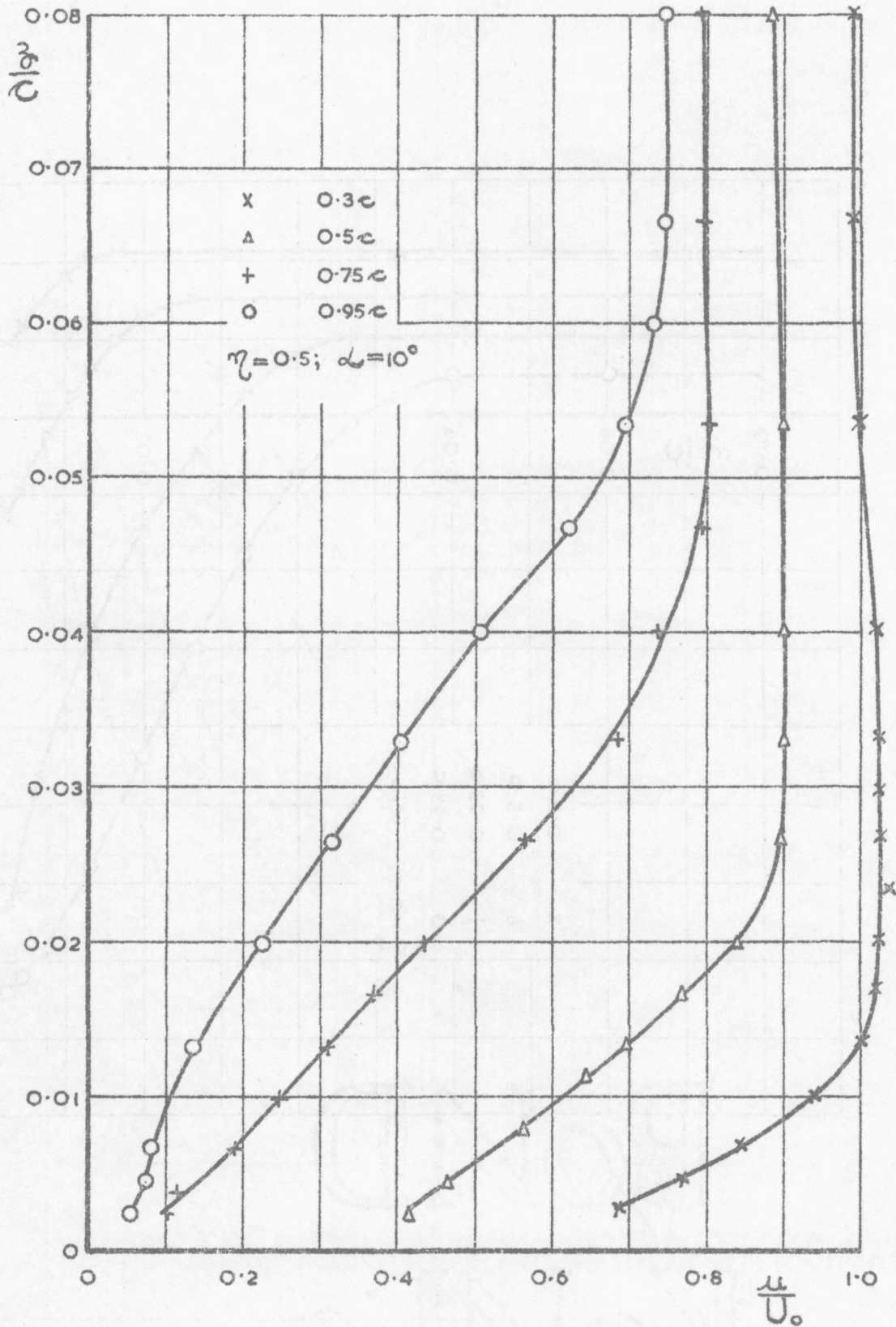


SPANWISE VELOCITY DISTRIBUTION THROUGH BOUNDARY LAYER.  
VARIATION WITH INCIDENCE.

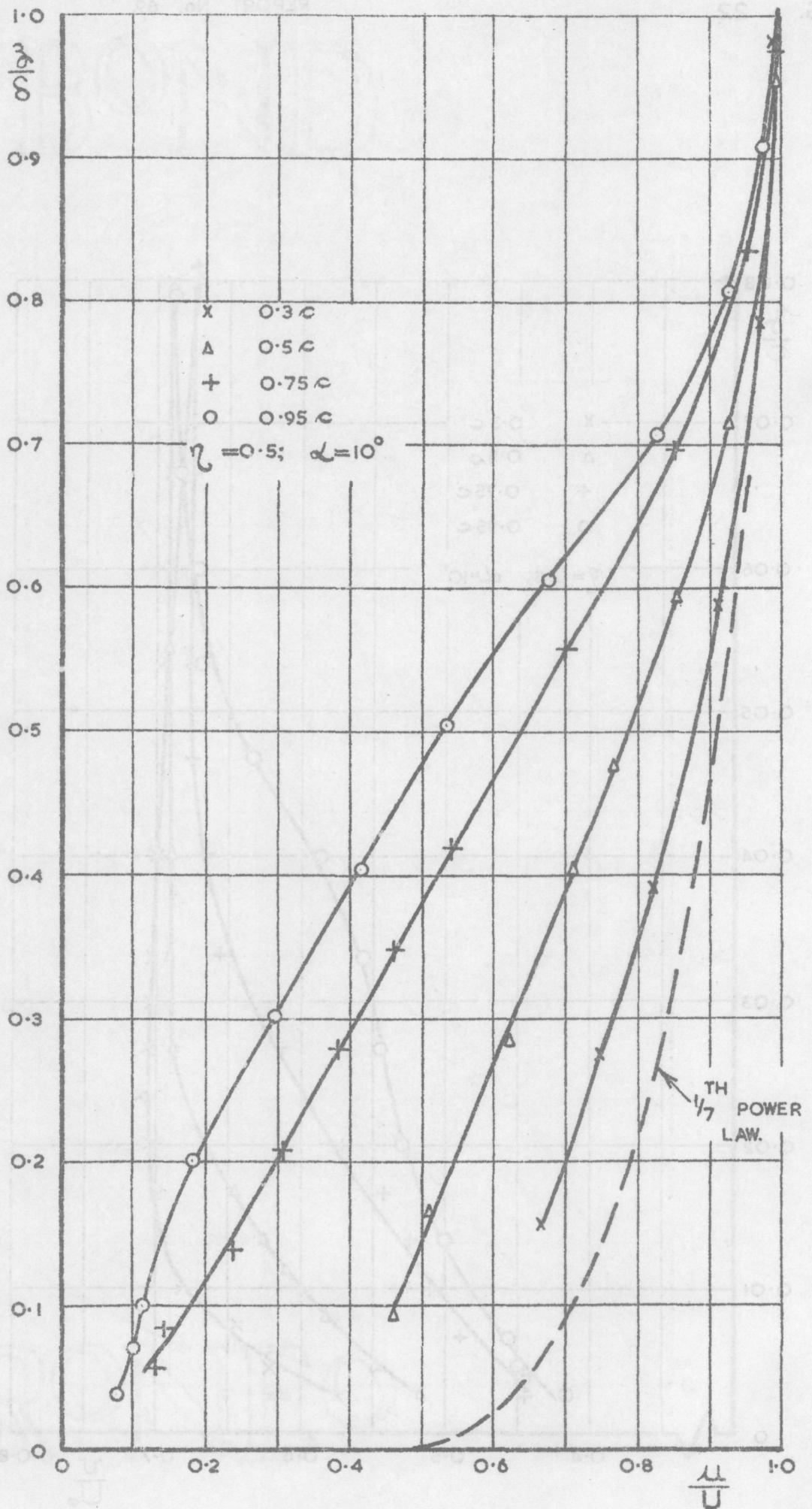


ANGLES OF FLOW THROUGH BOUNDARY LAYER.  
 VARIATION ACROSS CHORD.

FIG. 20.



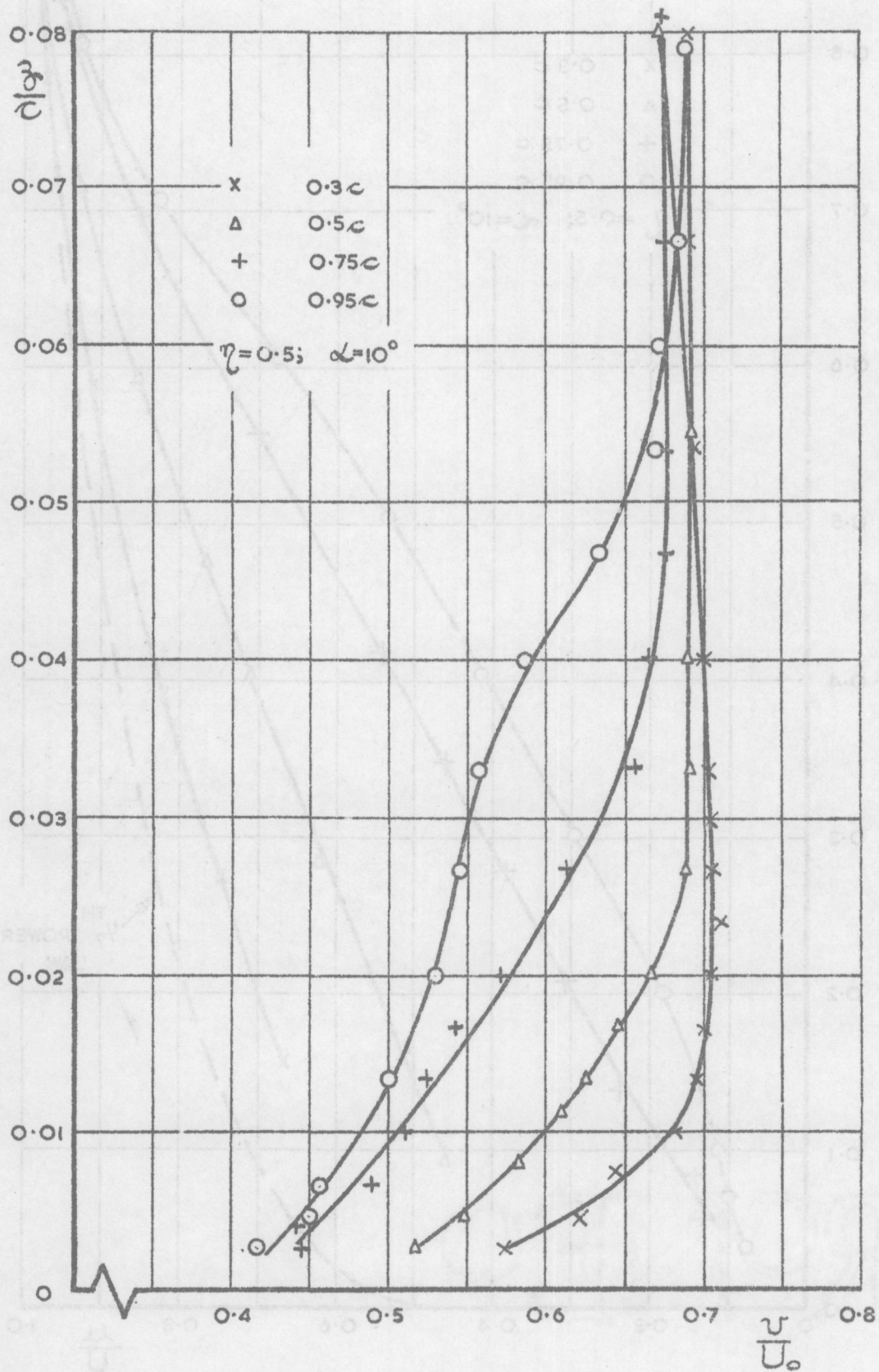
CHORDWISE VELOCITY DISTRIBUTION THROUGH BOUNDARY LAYER.  
 VARIATION ACROSS CHORD.



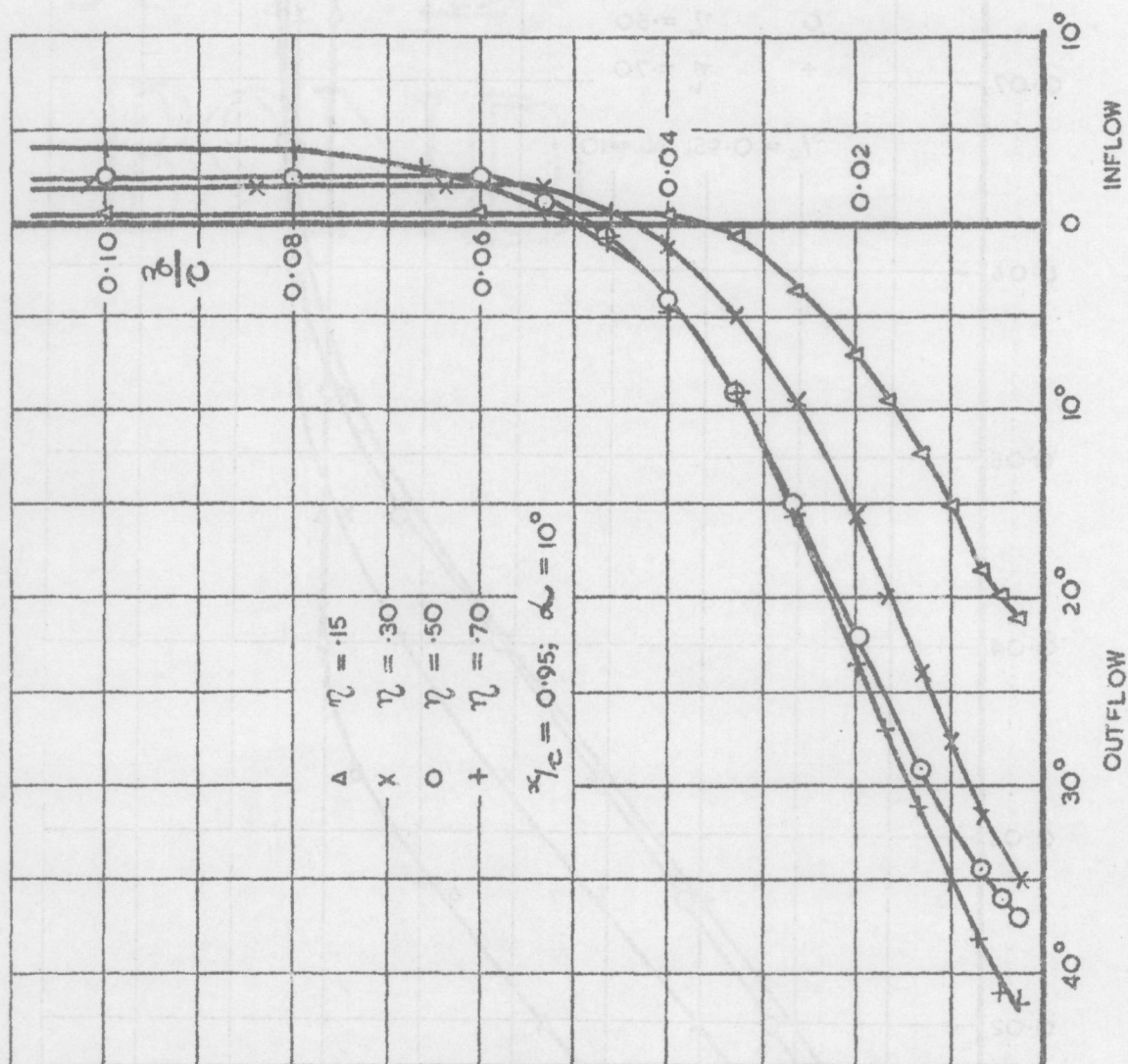
CHORDWISE BOUNDARY LAYER PROFILE.

VARIATION ACROSS CHORD.

FIG. 22.

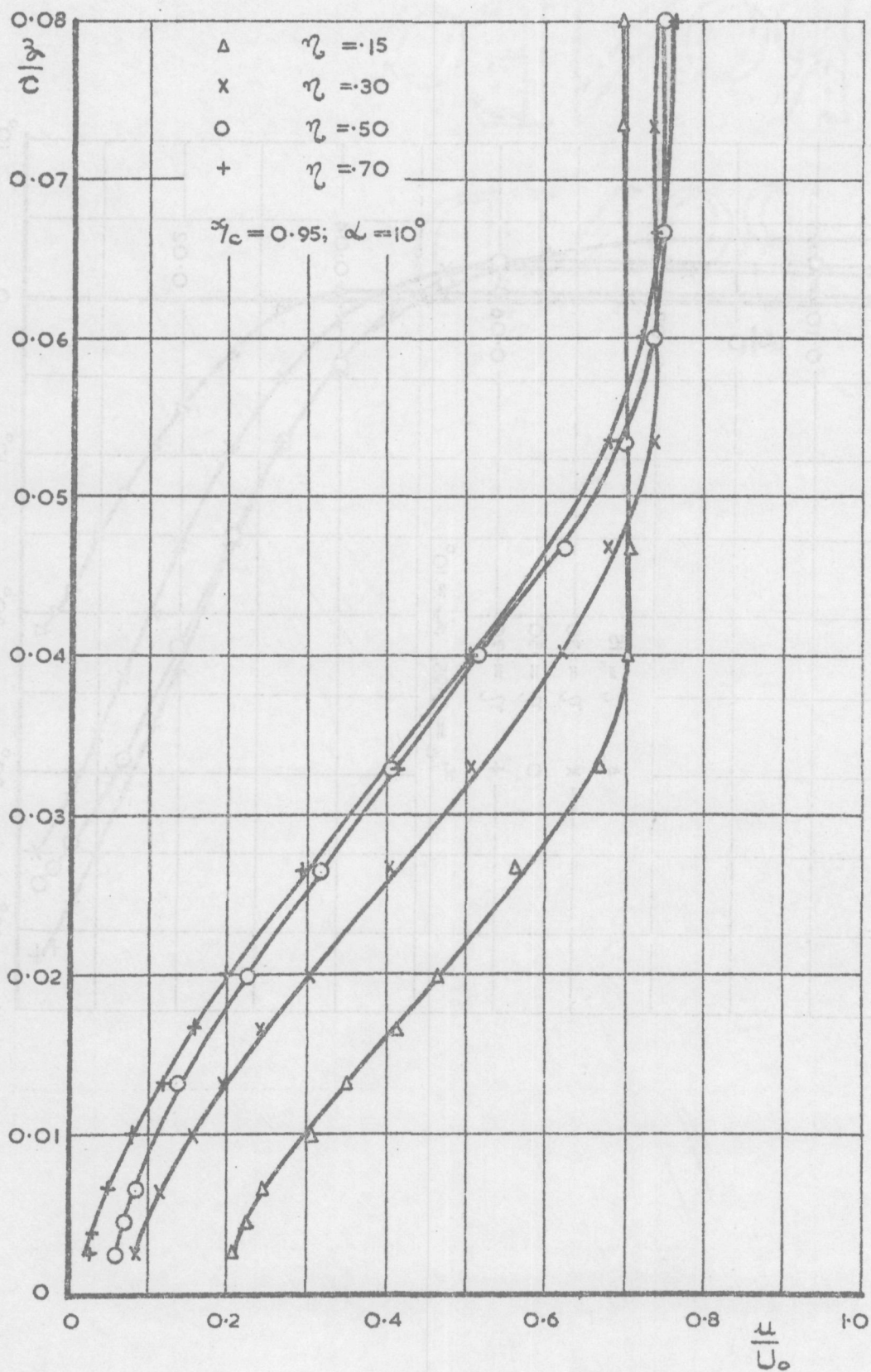


SPANWISE VELOCITY DISTRIBUTION THROUGH BOUNDARY LAYER.  
 VARIATION ACROSS CHORD.

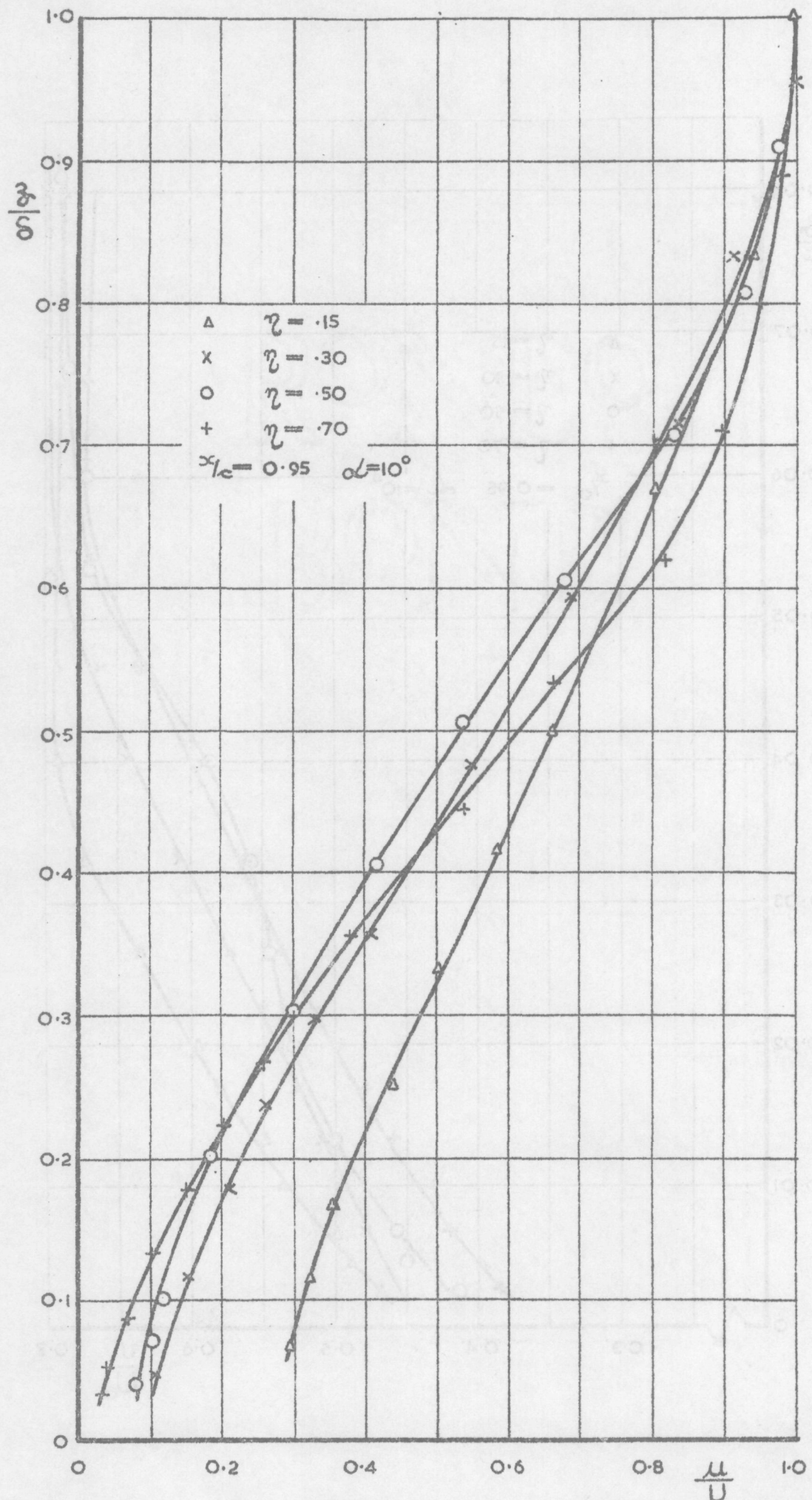


ANGLES OF FLOW THROUGH BOUNDARY LAYER.  
VARIATION ALONG SPAN.

FIG. 24.

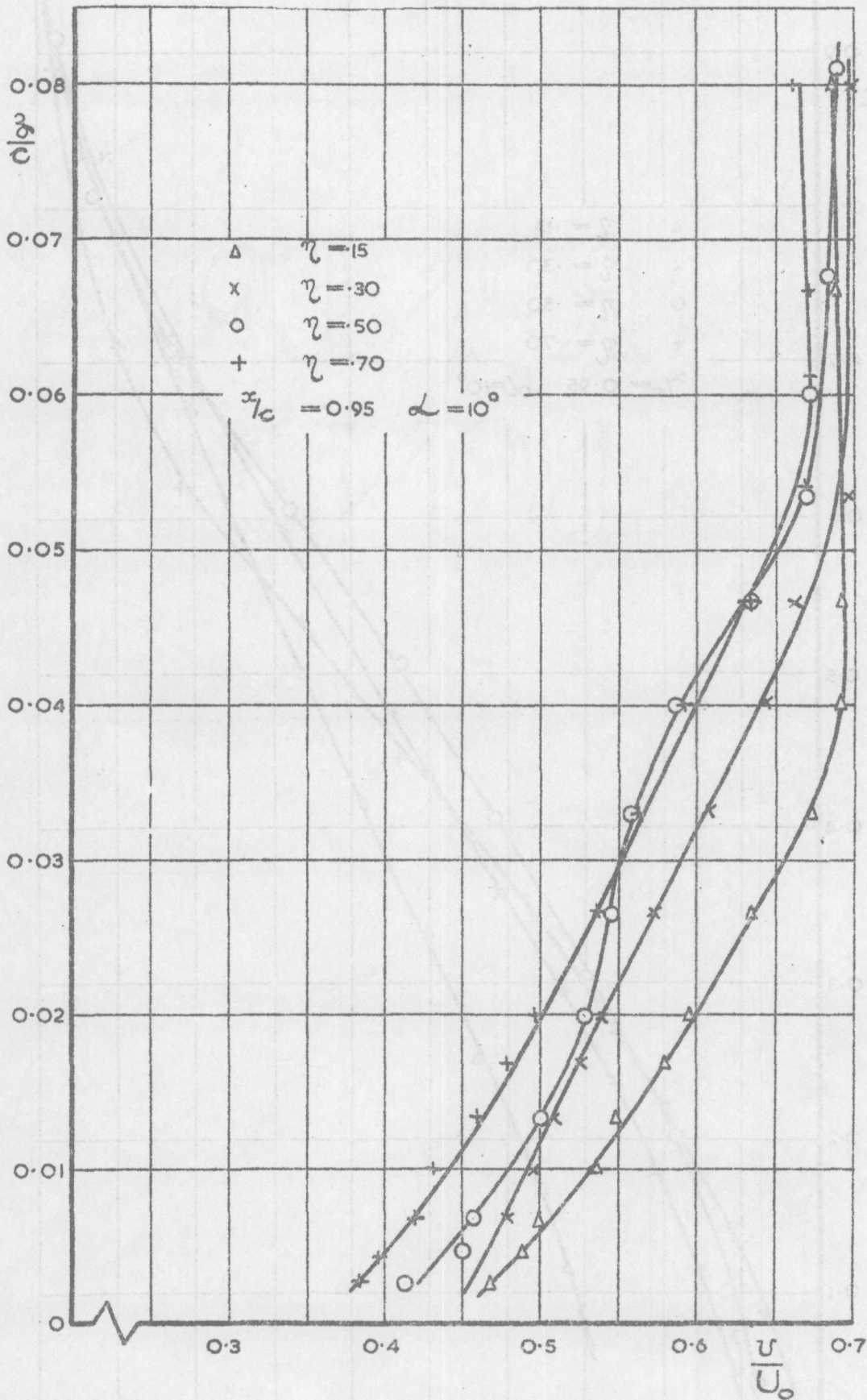


CHORDWISE VELOCITY DISTRIBUTION THROUGH BOUNDARY LAYER. VARIATION ALONG SPAN.



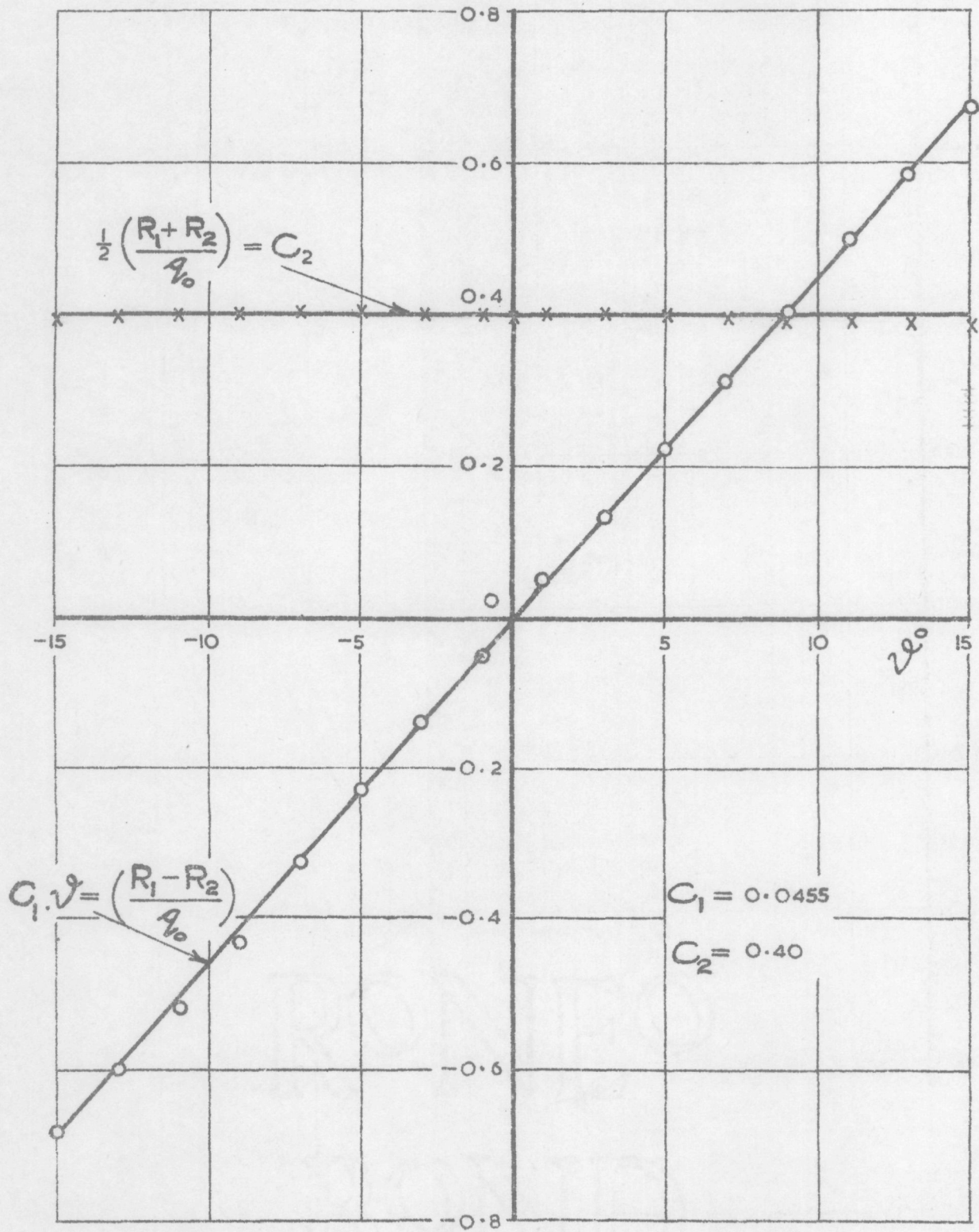
CHORDWISE BOUNDARY LAYER PROFILE, VARIATION ALONG SPAN.

FIG. 26.



SPANWISE VELOCITY DISTRIBUTION THROUGH BOUNDARY

LAYER. VARIATION ALONG SPAN.



CALIBRATION OF CONRAD YAWMETER.